Natural Resources for Human Health
eISSN: 2583-1194

Original Research

Received 20 July 2026
Revised 27 Aug 2026
Accepted 15 Sep 2026

Natural Resources for Human Health 2026, Vol. 6 (20s): 401–449

KEYWORDS:
Herbal Phytosomes, Asiatic acid, Bacopasaponin C, Drug delivery, Characterization, Nano carrier

Design, Development, and Characterization of Dual-Component Herbal Phytosomes of Asiatic Acid and Bacopasaponin C

Momin Subura Mohd Riyaz[1], Subur W Khan*[1], Dr. Rafiq Zakaria Campus

Y. B. Chavan College of Pharmacy, City-Aurangabad, Maharashtra, Country – India.
Email: samasubura47@gmail.com
ORCID: https://orcid.org/0009-0002-8797-1346
*Correspondence author: Subur W Khan
Email: suburkhan@yahoo.co.in
ORCID: https://orcid.org/0009-0001-5957-6560

ABSTRACT: Herbal phytosomes have emerged as promising nano-delivery systems for enhancing the bioavailability and therapeutic efficacy of poorly soluble phytoconstituents. Asiatic acid, a pentacyclic triterpene from Centella asiatica, and Bacopasaponin C, a bioactive saponin isolated from Bacopa monnieri, exhibit notable neuroprotective, antioxidant, and cognitive-enhancing activities; however, their clinical applicability is restricted by poor aqueous solubility, limited permeability, and low oral bioavailability. The present study aimed to formulate and evaluate dual-component herbal phytosomes containing Asiatic acid and Bacopasaponin C to improve their physicochemical and biopharmaceutical properties.

Preformulation investigations included determination of maximum wavelength, calibration curve development, and isobestic point analysis for both phytoconstituents. Simultaneous estimation was performed using RP-HPLC, demonstrating good linearity, precision, and specificity. Dual-component phytosomes were prepared by the antisolvent precipitation method employing phospholipids as vesicular carriers. The prepared phytosomes were evaluated for particle size, zeta potential, entrapment efficiency, drug content, and in vitro drug release. Structural and physicochemical characterization was conducted using FTIR, DSC, XRD, and SEM analyses.

The optimized phytosomal formulation exhibited nanosized vesicles with uniform distribution, satisfactory zeta potential, high entrapment efficiency, adequate drug content, and sustained release behavior. FTIR and DSC studies confirmed successful phytoconstituent-phospholipid complexation, while XRD revealed reduced crystallinity of the entrapped compounds. SEM analysis demonstrated nearly spherical vesicular structures. The developed phytosomal system significantly improved the physicochemical characteristics and delivery potential of both phytoconstituents.

The findings suggest that this nanoformulation may represent an effective strategy for improving stability, absorption, and therapeutic performance of herbal bioactives during administration.

Natural Resources for Human Health
eISSN: 2583-1194

1. INTRODUCTION

Herbal bioactive compounds have gained popularity in recent years due to their broad pharmacological characteristics and reasonably safe therapeutic profiles. However, the clinical utility of numerous phytoconstituents is frequently hampered by poor aqueous solubility, low permeability, instability, and insufficient bioavailability. These limitations considerably diminish their therapeutic efficacy when administered orally. To address these issues, innovative vesicular drug delivery technologies, such as phytosomes, have emerged as viable means to improving the physicochemical and biological properties of herbal substances [1,2].

Phytosomes are phospholipid-based vesicular systems in which phytoconstituents form molecular complexes with phospholipids, resulting in increased membrane permeability, absorption, and structural stability. Phytosomes have higher absorption and therapeutic potential than traditional herbal formulations due to their amphiphilic nature and nanosized vesicular structure [3]. Because of these advantages, phytosomal nanoformulations are becoming increasingly important in the fields of herbal medication delivery and nanomedicine.

Centella asiatica is a well-known medicinal herb that has traditionally been used in Ayurvedic medicine to treat neurological and cognitive issues. Asiatic acid, one of its main pentacyclic triterpenes compounds, has powerful antioxidant, anti-inflammatory, neuroprotective, and anticancer properties [4]. Nonetheless, its therapeutic potential is restricted by poor water solubility and oral absorption. Similarly, *Bacopa monnieri* is a valuable medicinal plant that has been shown to improve memory and protect the brain. Bacopasaponin C, a key bioactive saponin found in *Bacopa monnieri*, has been shown to improve cognitive function, protect neurons, and act as an antioxidant [5]. However, poor permeability and instability remain significant obstacles to its effective delivery. Asiatic acid and Bacopasaponin C may have synergistic therapeutic benefits due to their complementing neuroprotective and antioxidant effects. However, disadvantages such as poor solubility, instability, and low bioavailability may limit their efficacy in medicinal applications. To address these issues, the development of a dual-component phytosomal delivery system could be a promising strategy for improving the physicochemical stability and delivery capability of these phytoconstituents [6-10]. The current study intended to formulate, construct, and characterize herbal phytosomes containing Asiatic acid and Bacopasaponin C. The developed phytosomal system was subsequently evaluated for vesicular features, drug incorporation efficiency, release behavior, and overall physicochemical qualities to determine its feasibility as a possible nano-herbal delivery platform.

2. MATERIAL AND METHOD

2.1 Material

Asiatic acid was purchased from YUCCA Enterprises in Mumbai, Bacopasaponins C from BLD Pharma, soya lecithin from Yarrow Pharma, DCM (Dichloromethane) and N-Hexane from Fisher Scientific in Mumbai, and Methanol, Ethanol, N-Octanol, or DMSO (Dimethyl sulfoxide) from Loba. All of the other solvents and reagents were analytical grade.

2.2. Preformulation studies

2.2.1. Determination of Maximum wavelength (λmax) of Asiatic acid

The maximum wavelength (λmax) of Asiatic acid is determined using a UV-Visible spectrophotometer (Microprocessor double beam spectrophotometer LI-2702, Lasany). A standard solution is prepared by dissolving 10 mg of Asiatic acid in 100 mL of methanol to obtain a 100 µg/mL stock solution. Subsequently, a working solution of 10 µg/mL is prepared by appropriate dilution. The experimental procedure involved the use of a double-beam UV Visible spectrophotometer and quartz cuvettes to scan the sample over the wavelength range of 200-400 nanometers, with methanol serving as the blank. The resulting spectrum of absorbances is then recorded, and the wavelength at which the maximum absorption occurs is identified as the λmax [11].

2.2.2. Determination of Maximum wavelength (λmax) of Bacopasaponin C

In order to ascertain the maximum wavelength (λmax) of bacopasaponin, a UV-Visible spectrophotometer (Microprocessor double beam spectrophotometer LI-2702, Lasany) is employed. To this end, a standard solution is prepared by first dissolving 10 milligrams of bacopasaponin c in 100 milliliters of methanol or a methanol-water mixture. This results in a 100 µg/mL stock solution. Subsequently, a working solution of 10 µg/mL is prepared. The solution is scanned in the range of 200-400

nm using a UV-Visible double-beam spectrophotometer and quartz cuvettes, with the corresponding solvent serving as the blank. The resulting spectrum of absorbances is then recorded, and the wavelength at which the maximum absorption occurs is identified as the λmax [11].

2.2.3. Development of Calibration curve for Asiatic acid

The development of a calibration curve for Asiatic acid using a UV-Visible spectrophotometer (Microprocessor double beam spectrophotometer LI-2702, Lasany) entails the preparation of a standard stock solution. This solution is obtained by first dissolving 10 mg of Asiatic acid in 100 mg of methanol. The resultant solution is then filtered to ensure the removal of any particulate matter, and the concentration of the solution is recorded. The concentration of the solution is then calculated to be 100μg/ml. From this stock, a series of dilutions are made to prepare working solutions in the range of 2-12 μg/ml. Each solution is scanned at the previously determined λmax using a UV-Visible spectrophotometer with methanol as the blank. The absorbances of each concentration are measured, and a graph is plotted with absorbances on the Y-axis and concentrations on the X-axis. The resulting linear regression equation and correlation coefficient (R^2) confirm the linearity of the model and can be used for quantitative analysis [12].

2.2.4. Development of Calibration curve for Bacopasaponin C

The development of a calibration curve for Bacopasaponin c employs a UV-Visible spectrophotometer (Microprocessor double beam spectrophotometer LI-2702, Lasany), necessitating the preparation of a standard stock solution. This solution is attained by the dissolution of 10 mg of bacopasaponin c in 100 ml of methanol or a methanol: water (50:50) mixture, yielding a concentration of 100 μg/ml. From this stock, a series of working solutions in the range of 5-30 μg/ml are prepared by appropriate dilution. Each solution is scanned at the predetermined wavelength of Bacopasaponin using a UV-Visible spectrophotometer with the same solvent as the blank. The absorbances of each solution are recorded, and a calibration curve is constructed by plotting absorbances versus concentrations. The linearity of the curve is evaluated using linear regression analysis, and the correlation coefficient (R^2) is calculated to confirm the reliability of the method for quantitative estimation [12].

2.2.5. Isobestic point determination of Asiatic acid and Bacopasaponin C

The isosbestic point of Asiatic acid and Bacopasaponin c is determined using a UV-Visible spectrophotometer (Microprocessor double beam spectrophotometer LI-2702, Lasany). To do so, individual standard stock solutions of each compound are prepared (10 μg/mL). These solutions are prepared in methanol. From these, a series of working solutions with varying ratios of Asiatic acid to Bacopasaponin c (1:0, 3:1, 1:1, 1:3, 0:1) are prepared, maintaining a constant total concentration. Each solution was scanned in the UV range of 200-400 nm using a double-beam spectrophotometer with methanol as the blank. The resulting spectra were then overlaid, and the wavelength at which all spectra intersect was identified as the isosbestic point. This point is defined as the wavelength at which the total absorbance remains constant despite changes in component ratios.

2.2.6. Determination of RP HPLC standard and sample chromatogram of Asiatic acid

The quantification of Asiatic acid by RP-HPLC entails the preparation of a standard stock solution, which involves the dissolution of 10 mg of Asiatic acid in prepared mobile phase and subsequent dilution to 100 ml, yielding a concentration of 100 μg/ml. The mobile phase is typically composed of acetonitrile and water at a volumetric ratio of 70:30, with the pH adjusted to 3.0 using 0.1% orthophosphoric acid to ensure optimal peak resolution. The chromatographic separation is performed on a C18 column (250 mm × 4.6 mm, 5 μm) at a flow rate of 1.0 mL/min, with an injection volume of 20 μL and detection at 210 nm. Both standard and sample solutions undergo filtration through a 0.45 μm membrane filter prior to injection [13].

2.2.7. Determination of RP HPLC standard and sample chromatogram of Bacopasaponin C

The quantification of bacopasaponin c by RP-HPLC entails the preparation of a standard stock solution, which involves the dissolution of 10 mg of bacopasaponin c in a suitable mobile phase. The solution is then diluted to 100 ml, yielding a concentration of 100 μg/ml. The mobile phase is typically composed of acetonitrile and water, with a volumetric ratio of approximately 70:30, adjusted to a pH of approximately 3.0 using 0.1% orthophosphoric acid to enhance peak sharpness. The analysis is carried out using a C18 reverse-phase column (250 mm × 4.6 mm, 5 μm), with a flow rate of 1.0 mL/min, an

injection volume of 20 µL, and UV detection at a wavelength of 205 nm. All solutions are filtered through a 0.45 µm membrane filter prior to injection. Quantification is achieved through the comparison of the peak area of the sample with that of a standard prepared under analogous conditions [13].

2.2.8. Simultaneous determination of Asiatic acid and bacopasaponin C by using RPHPLC

The concurrent estimation of Asiatic acid and Bacopasaponin by RP-HPLC necessitates the preparation of standard stock solutions for each compound (10 mg in 100 mL methanol, yielding 100 µg/mL) and the subsequent generation of suitable sample solutions from formulations. The mobile phase is typically composed of acetonitrile and water, with a ratio of 70:30 (v/v), adjusted to a pH of 3.0 using 0.1% orthophosphoric acid to enhance peak resolution. The chromatographic separation is carried out using a C18 column (250 mm × 4.6 mm, 5 µm) at a flow rate of 1.0 mL/min, with an injection volume of 20 µL and detection at 245 nm. All solutions are filtered through a 0.45 µm membrane before injection.

2.2.9. FTIR Analysis

Fourier transform infrared (FTIR) studies were carried out using the KBr pellet method. Briefly, dried potassium bromide (KBr), phytoconstituents, and soya lecithin (phosphatidylcholine) were accurately weighed, blended, and compressed to obtain pellets. The prepared pellet was placed in the sample holder, and spectra were recorded over a scanning range of 4000-400 cm^{-1}. FTIR spectra of the phytoconstituents and excipient were obtained using a Jasco FTIR-4100, Japan spectrophotometer at MIT College, Aurangabad, India [14].

2.3 Experimental Design and Optimization of Phytosomes

Eight different batches of phytosomes (B1-B8) were initially prepared by varying the concentration of soya lecithin, reaction temperature, and reaction time, while maintaining constant amounts of asiatic acid and Bacopasaponin c. Each batch contained 50 mg of asiatic acid and 50 mg of Bacopasaponin c. The Composition of all designed batches was presented in Table S1. All prepared formulations (B1-B8) were evaluated for physicochemical characteristics including particle size, entrapment efficiency, and stability. A 2^3 full factorial design was employed to investigate the influence of three independent variables on the formulation of phytosomes containing asiatic acid and Bacopasaponin c. The three independent factors studied were concentration of soya lecithin (A), reaction temperature (B), and reaction time (C). The design consisted of eight experimental runs representing all possible combinations of the selected variables at two levels (low and high). The experimental runs were randomized to minimize potential experimental bias. A three-factor interaction (3FI) model was selected to assess the main effects, two-factor interaction effects, and three-factor interaction effects of the independent variables on the measured responses. The factorial design matrix and corresponding responses are provided in Table S2. Further optimization of the phytosomal system was carried out using Design-Expert® software (Version 13.0.5.0). A three-factor response surface design was used to evaluate the effects of concentration of soya lecithin, reaction temperature, and reaction time on the responses of the developed phytosomes. The experimental design included factorial points, axial points, and replicated center points, resulting in a total of 57 experimental runs with different combinations of the selected variables. All experimental formulations were analyzed to determine the optimum processing conditions for achieving minimum particle size and maximum drug release, and the formulation exhibiting the most desirable characteristics was selected as the optimized batch for further studies.

2.3.1. Preparation of Optimized Asiatic Acid-Bacopasaponin C Phytosomes

Based on the optimization study, the final optimized phytosomal formulation containing asiatic acid and Bacopasaponin c was prepared under the selected processing conditions using the antisolvent precipitation technique. The accurately weighed phospholipid was dissolved in dichloromethane (DCM) and transferred to a round-bottom flask. The drug components were separately dissolved in an appropriate solvent system and then added to the phospholipid solution. The resulting mixture was refluxed at 50 °C for 2 h to facilitate complex formation. Following reflux, the solvent volume was reduced, after which n-hexane was gradually added under continuous stirring to induce precipitation of the phytosomal complex. The resulting dispersion was further subjected to probe sonication for eight cycles of 30 s each to obtain a uniform phytosomal suspension for subsequent characterization and evaluation.

2.4 Physicochemical Evaluation of Optimized Asiatic Acid-Bacopasaponin C Phytosomes

2.4.1. Particle size and zeta potential

The particle size and zeta potential of the optimized phytosomal formulation comprising asiatic acid and bacopasaponin c were measured with a Malvern Panalytical zeta potential analyzer. Prior to measurement, the formulation was diluted with double-distilled water to achieve the desired concentration for analysis. The diluted sample was tested for particle size distribution and zeta potential under regular working conditions [15].

2.4.2. Entrapment efficiency

The entrapment efficiency of asiatic acid and bacopasaponin c in the optimized phytosomal formulation was measured using ultracentrifugation. Entrapment efficiency is the percentage of drugs encapsulated or connected with phytosomal vesicles. 1 mL of the phytosomal dispersion was transferred to a volumetric flask, diluted with phosphate buffer (pH 6.8), and the volume adjusted to 10 mL. The diluted sample was then centrifuged at 15,000 rpm for 60 minutes to separate the entrapped and free drug fractions. The supernatant was filtered through a 0.22 μm membrane filter and absorbance was measured using a UV-Visible spectrophotometer at 282 nm to estimate the amount of unentrapped medication [15].

2.4.3. Drug content analysis

The phytosomal suspension was dissolved in 100 mL of phosphate buffer (pH 6.8) and constantly swirled for 2 hours using a magnetic stirrer. The resultant solution was then filtered, with 1 mL of the filtrate removed and diluted to 10 mL in a volumetric flask. The sample solution's absorbance was then measured using a UV spectrophotometer at 282 nm [15].

2.4.4. In vitro release study

Drug release from phytosomes was assessed using the dialysis membrane method. The dissolution media included a 0.1 N HCl solution and phosphate buffer (pH 6.8). The complete assembly was placed on a magnetic stirrer, and the temperature was kept at 37°C by continuously stirring with a magnetic bead. The dissolution investigation was conducted using 0.1 N HCl for the first 2 hours, followed by phosphate buffer (pH 6.8) for the next 10 hours. To maintain sink conditions, 1 mL of the dissolution medium was taken at regular intervals and replaced with an equivalent volume of fresh media. The collected samples were examined with a UV spectrophotometer at 282 nm, and the cumulative drug release (% CDR) was estimated [15].

2.4.5. Differential scanning calorimetry (DSC) analysis

The thermal examination of the materials asiatic acid and Bacopasaponin c, phospholipid (Soya lecithin), physical mixture, and produced phytosomes was performed using a Differential Scanning Calorimeter (Shimadzu DSC-60). Samples were analyzed in crimped aluminum pans heated at 30-500°C at a heating rate of 10°C min-1 to test the purity of drug results obtained when compared to the literature record [15].

2.4.6. Scanning electron microscopy (SEM) analysis

Scanning electron microscopy (SEM) was used to analyze the phytosomal formulation's particle size and surface appearance. The dried sample was mounted on a gold-coated brass stub and studied using a scanning electron microscope (JEOL JSM-6360). Digital micrographs of the phytosomal complex were acquired by random scanning of the stub at magnifications of 3000× and 5000×(5) [15].

2.4.7. XRD Analysis

XRD evaluation was carried out on pure phytoconstituents and optimized formulation using Shimadzu XRD-7000 diffractometer (Tokyo, Japan) equipped with a scan step rate of 2^{o}/min over a 20range of 5^{o} to 60^{o} [15].

3. RESULTS AND DISCUSSION

3.1. Maximum wavelength (λmax) determination of Asiatic acid

A UV-visible spectrophotometric analysis of asiatic acid was performed using methanol as the solvent. A standard solution of 10 μg/mL Asiatic acid was scanned over a wavelength range of 200-400 nm using a double-beam UV-visible

spectrophotometer. The absorbance spectrum showed a distinct peak in (Fig. S1A), with the maximum absorbance observed at 282 nm. This indicates that 282 nm is the λ_(max) of Asiatic acid under these experimental conditions. This wavelength will be used for further quantitative estimation and calibration curve development.

3.2. Maximum wavelength (λmax) determination of Bacopasaponin C

A UV-visible spectrophotometric scan of Bacopasaponin c was performed using methanol as the solvent. A standard Bacopasaponin c solution (10 µg/mL) was scanned from 200 to 400 nm using a double-beam UV-visible spectrophotometer. The absorbance spectrum exhibited a clear peak in (fig. S1B), with maximum absorbance observed at 273 nm, identified as the λ(max) of Bacopasaponin c. This wavelength will be used for further analytical evaluations, including constructing a calibration curve and performing simultaneous estimation studies.

3.3. Isobestic point determination of Asiatic acid and Bacopasaponin C

We determined the isosbestic point of asiatic acid and Bacopasaponin c by scanning the UV absorbance spectra of individual solutions and mixtures of varying ratios over the range of 200-400 nm, using methanol as the solvent. Absorbance values were recorded at multiple wavelengths and plotted to identify the overlapping region. The absorbance spectra of Asiatic acid and Bacopasaponin c, as well as their 1:1 mixture, consistently intersected at a common wavelength, confirming the presence of an isosbestic point as shown in (Fig. S1C).

This intersection occurred at approximately 277 nm, indicating that this wavelength is the isosbestic point for the two compounds. The black colour graph showing the wavelength at near about 273 nm which is maximum wavelength of asiatic acid whereas red colour graph showed maximum wavelength of Bacopasaponin c at near 282 nm. This wavelength reflects a region in which both compounds have equal absorbance, making it suitable for their simultaneous estimation under specific analytical conditions.

3.4. Development of Calibration curve for Asiatic acid

A calibration curve for asiatic acid was developed using UV-visible spectrophotometry at its maximum absorption wavelength (λ_(max)) of 273 nm in methanol. Standard solutions were prepared in the concentration range of 2-12 µg/mL, and their absorbance values were recorded. The absorbance increased linearly with concentration, yielding the following regression equation: y=mx+c (0.0979x+0.053) with a high correlation coefficient (R^2 = 0.999) (Fig. S2A), Table S3. This indicates excellent linearity. These results confirm compliance with the Beer-Lambert law, establishing the method as suitable for quantitatively estimating Asiatic acid.

3.5. Development of Calibration curve for Bacopasaponin C

We developed a calibration curve for Bacopasaponin c using UV-Vis spectrophotometry at its maximum absorption wavelength λ(max), which is typically observed around 273 nm in methanol. Standard solutions of Bacopasaponin c were prepared in the concentration range of 5-30 µg/mL, and their absorbance was measured. The absorbance values exhibited a strong linear relationship with concentration, yielding a regression equation of absorbance y= 0.0398x-0.1384, with a correlation coefficient (R^2) of 0.999 (Fig. S2B), Table S4. This indicates good linearity. These results confirm the reliability of this method for quantitatively estimating Bacopasaponin c using UV-Vis analysis.

3.6. Determination of RP HPLC standard and sample chromatogram of Asiatic acid

Determination of Asiatic acid using a C18 column and UV detection was carried out. Standard solutions of Asiatic acid and standard/sample solutions were analyzed under optimized chromatographic conditions. The mobile phase consisted of acetonitrile and water (pH with 0.1% orthophosphoric acid) at a ratio of 70:30 (v/v). The flow rate was set at 1.0 mL/min, and detection was carried out at λ max 210 nm. The retention time (Rt) of Asiatic acid was found to be approximately 6.253 min in the standard and sample retention time 6.183 min was chromatograms, confirming its presence in the sample [16]. The chromatograms displayed sharp, symmetric peaks with good resolution. The standard chromatogram displayed a single, well-resolved peak for asiatic acid. The sample chromatogram showed an additional peak at the same retention time, indicating accurate identification (Fig. S3A-B).

3.7. Determination of RP HPLC standard and sample chromatogram of Bacopasaponin C

Determination of Bacopasaponin c using a reverse-phase C18 column and UV detection was carried out. Optimized chromatographic conditions included a mobile phase of volumetric ratio of approximately 70:30, adjusted to a pH of approximately 3.0 using 0.1% orthophosphoric acid, a flow rate of 1.0 mL/min, and UV detection at 205 nm. Standard and sample solutions were injected, each showing a sharp, well-resolved peak. Bacopasaponin c retention time (Rt) was observed at 12.782 min in standard and sample chromatograms (Fig. S4A-B). The sample chromatogram exhibited a peak at the same Rt, confirming the presence of Bacopasaponin c [16].

3.8. Simultaneous determination of Asiatic acid and Bacopasaponin c by using RPHPLC

Standard and sample solutions containing both compounds were injected, and well-resolved, sharp peaks were observed (Fig. S5A-B). Asiatic acid eluted at a retention time (Rt) of approximately 6.285min, and Bacopasaponin c at around 12.736 min, with no interference between the two peaks [17].

3.9. Drug content analysis

The drug content of the phytosomal formulations ranged from 82.48% to 93.12%, which indicates the efficient incorporation of the Asiatic acid and Bacopasaponin C into the phospholipid matrix. Batch B7 had the highest drug content because of optimal formulation conditions, such as a lower lecithin concentration, a higher temperature, and an extended reaction time. These conditions facilitated effective complexation. Conversely, formulations with a higher lecithin concentration had relatively lower drug content, likely due to aggregation and reduced drug entrapment efficiency. Temperature and time were found to significantly enhance drug incorporation by promoting better interaction between drug molecules and phospholipids, Table S5.

3.10. Determination of entrapment efficiency

The entrapment efficiency of phytosomal formulations ranged from 71.22% to 88.96%, indicating effective incorporation of Asiatic acid and Bacopasaponin C within the phospholipid matrix, Table S6.

Batch B7 demonstrated the highest entrapment efficiency, attributable to the optimal combination of reduced lecithin concentration, elevated temperature, and protracted reaction time, thereby enhancing drug phospholipid complexation. Conversely, formulations with higher lecithin concentrations exhibited diminished entrapment efficiency, a phenomenon that may be attributed to vesicle aggregation and diminished drug accommodation capacity. The findings of this study demonstrated that temperature and reaction time exerted a substantial influence on entrapment efficiency, thereby facilitating enhanced interaction between the drug and phospholipid.

3.11. Determination of Particle Size

The particle size of phytosomal formulations ranged from 246.14 nm to 498.06 nm, indicating successful formation of nanosized vesicular systems, (Fig. S6A-H) and Table S7.

Batch B7 exhibited the smallest particle size due to the combined effect of lower lecithin concentration, higher temperature, and extended reaction time, which facilitated efficient phytosome formation. Conversely, batch B8 exhibited the most substantial particle size, a phenomenon attributable to elevated lecithin levels in conjunction with reduced temperature and abbreviated reaction time. This combination resulted in aggregation and incomplete complexation. In summary, an increase in lecithin concentration resulted in an increase in vesicle size. Conversely, higher temperature and longer reaction time contributed to a reduction in particle size.

3.12. Determination of Zeta Potential

The zeta potential of phytosomal formulations ranged from -22.73 mV to -34.67 mV, indicating moderate to good stability of the vesicular system. Batch B7 demonstrated the highest zeta potential, indicating optimal colloidal stability under ideal formulation conditions, namely lower lecithin concentration, elevated temperature, and protracted reaction time, (Fig. S7A-H) and Table S8.

Conversely, batch B8 exhibited the lowest zeta potential, suggesting suboptimal stability and a propensity for aggregation. Increased lecithin concentration was found to reduce effective surface charge, while higher temperature and longer reaction time improved zeta potential by promoting better organization of the phospholipid bilayer.

***3.13. In Vitro* release Study**

The *in-vitro* dissolution study demonstrated that all phytosomal formulations exhibited a biphasic release pattern, with an initial burst followed by sustained release up to 24 hours. The release of the drug was found to be significantly influenced by the concentration of lecithin, the temperature, and the reaction time. An elevated level of lecithin has been demonstrated to impede the release of drugs due to the establishment of a more substantial lipid barrier (Fig. 1) and Table S9.

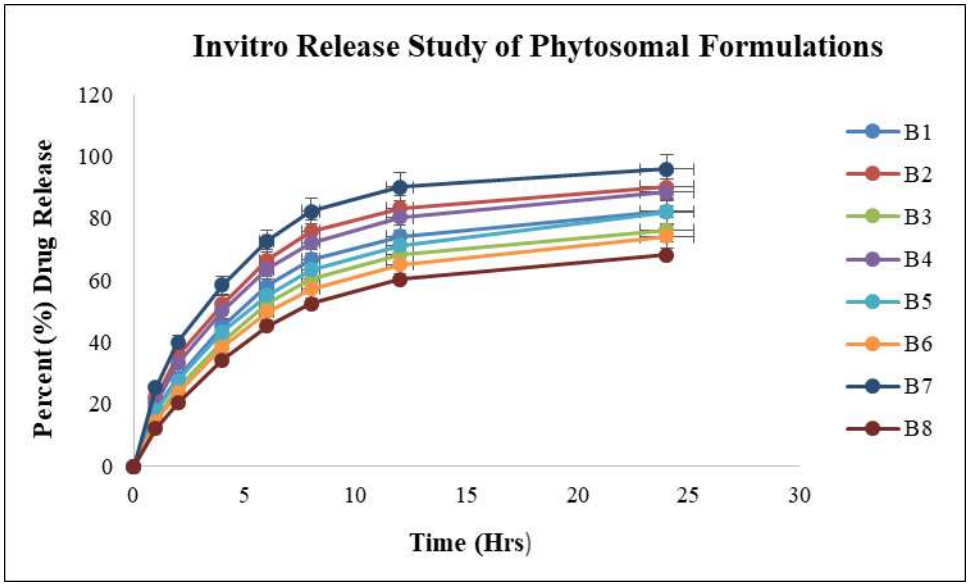


Fig. 1. *In vitro* release graph of phytosomal formulation

Conversely, an escalation in both temperature and reaction time has been shown to promote the release process by enhancing phytosome formation and concurrently reducing particle size. Batch B7 was identified as the optimized formulation, demonstrating maximum drug release. This phenomenon can be attributed to its optimal composition and processing conditions. The release kinetics indicated a diffusion-controlled mechanism, suggesting the potential of phytosomes for sustained drug delivery.

3.14. Build Information

A 2^3 full factorial design was utilized to investigate the impact of three independent variables on the formulation of phytosomes containing Asiatic acid and Bacopasaponin C. The experimental design comprised eight runs, encompassing all possible combinations of the selected factors at two levels (low and high). The experimental design was subjected to a randomization process to mitigate the potential for experimental bias. A three-factor interaction (3FI) model was selected to evaluate the main effects, two-factor interactions, and three-factor interaction effects on the response variables Table S10.

3.15. Factors

For the factorial design, three independent variables were selected: concentration of soya lecithin (A), temperature (B), and reaction time (C). Each factor was studied at two levels, coded as -1 (low) and +1 (high). The concentration of soya lecithin was varied from 100 to 200 mg, the temperature from 50 to 70℃, and the reaction time from 90 to 150 min. All variables were treated as numeric and continuous. The midpoint values were established at 150 mg, 60 ℃, and 120 min, respectively. The independent variables selected for the factorial design included concentration of soya lecithin, temperature, and reaction time. These were studied as continuous numeric factors. The selection of these ranges was informed by preliminary trials, which were conducted to ensure the effective formation of phytosomes without compromising their stability. The broad spectrum of lecithin concentrations enabled the assessment of its effect on vesicle formation, while temperature and duration were meticulously calibrated to amplify the interaction between drugs and phospholipids, Table S11. The variability observed in experimental responses indicates that these factors significantly influenced the physicochemical characteristics of the phytosomal formulations.

3.15.1. Response 1 - Particle Size

The Pareto chart for particle size (Fig. S8) indicates that Factor A (concentration of soya lecithin) exerts the most significant influence on particle size, as evidenced by its highest t-value among all effects. The chart demonstrates a positive effect, meaning that increasing lecithin concentration leads to an increase in particle size.

This phenomenon is substantiated by scientific evidence, which attributes the observed effects to the accumulation of thicker phospholipid bilayers and the potential aggregation of vesicles at higher lipid content. Conversely, factors C (time) and B (temperature) demonstrate a negative effect, suggesting that an increase in reaction time and temperature leads to a decrease in particle size. This phenomenon is likely attributable to enhanced molecular interaction and improved phytosome formation efficiency. Among these factors, time has been shown to exert a more pronounced effect than temperature, indicating that extended processing is more critical for achieving smaller and more uniform vesicles. The interaction terms (AB, BC, AC) and the three-factor interaction (ABC) display comparatively very low t-values, falling below the significance threshold. This indicates that their combined effects are minimal and statistically insignificant in influencing particle size. Furthermore, none of the factors exceed the Bonferroni limit; however, the main effects (A, B, and C) surpass the t-value threshold, thereby confirming their status as the predominant contributors. The analysis demonstrates that particle size is primarily governed by lecithin concentration, with process variables such as temperature and time playing supportive but significant roles in size reduction.

3.16. ANOVA for selected factorial model

3.16.1. Response 1: Particle Size

The results of the analysis of variance (ANOVA) for particle size evidently demonstrate that the overall model is statistically significant ($F = 667.01$, $p = 0.0296$), indicating that the selected factors collectively exert a strong influence on the response. Among the individual factors, Factor A (concentration of soya lecithin) demonstrates the highest degree of contribution (Sum of Squares = 17605.32, $F = 1590.58$, $p = 0.0160$), substantiating its role as the predominant variable affecting particle size, with elevated concentrations resulting in augmented vesicle size due to enhanced lipid bilayer formation. Factor C (time) also exhibited a highly significant effect ($F = 1456.71$, $p = 0.0167$), suggesting that increased reaction time plays a crucial role in reducing particle size by promoting complete phytosome formation and uniformity, Table S12.

In a similar vein, Factor B (temperature) exhibited a substantial impact on the response ($F = 902.23$, $p = 0.0212$), suggesting that elevated temperatures facilitate enhanced molecular interaction and a reduction in particle size. Conversely, the interaction terms AB, AC, and BC exhibited p-values (>0.05) that were comparatively elevated, suggesting that these interactions are statistically insignificant and do not contribute substantially to the variation in particle size. The model's excellent fit is further substantiated by the minimal unexplained variation, as evidenced by the very low residual error (Sum of Squares = 11.07). The analysis indicates that the predominant factors influencing particle size are lecithin concentration, temperature, and time, with minimal interaction effects. This finding substantiates the robustness and reliability of the factorial design model.

3.16.2. Fit Statistics

The statistical parameters of the model indicate an excellent fit and high reliability of the factorial design. The standard deviation (3.33) is minimal, indicating negligible variation between experimental and predicted values, which suggests that the model is precise. The coefficient of variation (C.V. = 0.8619%) is well below 10%, indicating high reproducibility and reliability of the experimental data, Table S13.

The R^2 value (0.9998) indicates that 99.98% of the variability in particle size is explained by the model, confirming an almost perfect fit. This conclusion is further substantiated by the adjusted R^2 value of 0.9983, which is nearly equivalent to the original R^2, suggesting that the model has not been overfitted and that all incorporated terms are significant. Furthermore, the predicted R^2 (0.9840) is reasonably aligned with the adjusted R^2 (difference < 0.2), thereby substantiating the model's substantial predictive capacity for novel observations. The Adeq Precision value (81.7054), which is considerably higher than the requisite minimum of 4, signifies an adequate signal-to-noise ratio, thereby validating the model's efficacy in navigating the design space. The statistical indicators demonstrate the model's robustness, precision, and suitability for optimization and prediction of particle size in phytosomal formulations.

3.16.3. Coefficients in Terms of Coded Factors

The regression coefficients, expressed in terms of coded factors, offer a quantitative understanding of how each variable influences particle size. The model demonstrates strong statistical reliability. The intercept (386.02) is indicative of the average particle size at the midpoint levels of all factors. Among the primary effects, Factor A (concentration of soya lecithin) demonstrates a substantial positive coefficient (+46.91), signifying that an augmentation in lecithin concentration results in a considerable enhancement in particle size. This outcome is in accordance with the promotion of enhanced lipid bilayer formation and vesicle aggregation. In contrast, factors B (temperature) and C (time) exhibited negative coefficients of -35.33 and -44.89, respectively, indicating that increases in temperature and time result in a reduction in particle size due to enhanced molecular interaction and more efficient phytosome formation, Table S14.

It is noteworthy that Factor C exerts a marginally more pronounced effect than Factor B, indicating that reaction time is a more significant factor in the reduction of size. The interaction terms AB (+4.63), AC (+2.63), and BC (-6.66) have relatively small coefficients, and their confidence intervals include zero. This indicates that these interactions are statistically insignificant and have minimal practical impact on particle size. Furthermore, the Variance Inflation Factor (VIF = 1.000 for all terms) verifies the absence of multi collinearity, indicating that all factors are independent and the model estimates are reliable. The coefficient analysis indicates that the primary factors influencing particle size are lecithin concentration, followed by time and temperature. This analysis validates the model's robustness and interpretability, as interaction effects are found to be negligible.

3.16.4. Final Equation in Terms of Coded Factors

The final regression equation, expressed in terms of coded factors, provides a quantitative description of the relationship between formulation variables and particle size. This equation clearly indicates the magnitude and direction of each effect. The positive coefficient of Factor A (+46.91) confirms that increasing the concentration of soya lecithin significantly increases particle size, thereby making it the most dominant factor in the model due to its highest coefficient value. In contrast, factors B (temperature, -35.33) and C (time, -44.89) exhibit negative coefficients, indicating that increasing temperature and reaction time leads to a reduction in particle size, with time having a slightly stronger impact than temperature. This finding indicates that extended processing enhances phytosome formation and reduces vesicle size more efficiently. The interaction terms AB (+4.63), AC (+2.63), and BC (-6.66) have comparatively small coefficients, indicating minimal interaction effects. However, the negative BC term suggests a slight synergistic effect between temperature and time in reducing particle size.

Particle size = +386.02+46.91*A-35.33*B-44.89*C+4.63*AB+2.63*AC-6.66*BC

The comparatively larger magnitude of the main effects in relation to the interaction terms indicates that particle size is predominantly governed by individual factors as opposed to their combinations. The equation demonstrates that optimal particle size can be achieved by maintaining lower lecithin concentration while increasing temperature and reaction time. It can be used to effectively predict and optimize formulation conditions within the studied design space.

3.16.5. Final Equation in Terms of Actual Factors

The final equation, in terms of actual factors, provides a practical and quantitative relationship between formulation variables and particle size, allowing for direct prediction within the experimental range.

Particle Size= +591.91500+0.172375*Concentration of Soya Lecithin-2.25750* Temperature-0.428083*Time+0.009253*Concentration of Soya Lecithin*Temperature+0.001756*Concentration of Soya Lecithin * Time-0.022196Temperature * Time

The positive coefficient for concentration of soya lecithin (+0.172375) indicates that an increase in lecithin concentration leads to a proportional increase in particle size, confirming its dominant role in vesicle enlargement due to thicker lipid bilayer formation. Conversely, temperature (β = -2.25750) and time (β = -0.428083) exhibited negative coefficients, suggesting that increasing these process parameters led to a substantial reduction in particle size. Notably, temperature exerted a more pronounced effect compared to time, which may be attributed to enhanced molecular mobility and enhanced drug–phospholipid interaction at elevated temperatures. The interaction term between lecithin and temperature (+0.009253) suggests a slight synergistic effect that increases particle size when both variables are increased simultaneously, whereas the

interaction between lecithin and time (+0.001756) shows a very minimal positive contribution, indicating negligible practical influence. Conversely, the negative interaction between temperature and time (-0.022196) indicates a combined effect that further reduces particle size when both parameters are increased together, highlighting a synergistic role in promoting efficient phytosome formation. The equation indicates that particle size is predominantly influenced by lecithin concentration (exhibiting an increasing effect) and temperature (exhibiting a strong decreasing effect), with time contributing moderately. It functions as a reliable predictive tool for optimizing formulation conditions within the studied design space.

3.16.6. Normal Plot of Residual

The standard plot of residuals for particle size indicates that the developed model satisfies the key assumption of normality of residuals (Fig. S9), which is essential for the validity of ANOVA and regression analysis. The data points are observed to fall approximately along a straight vertical alignment, with no systematic deviation or curvature. This suggests that the residuals are randomly and normally distributed.

The absence of extreme outliers or points deviating significantly from the trend suggests the absence of abnormal experimental errors or influential observations. Furthermore, the distribution of residuals appears to be uniform across the range, suggesting homoscedasticity (constant variance) of errors. The color coding, which represents particle size values from lower (blue) to higher (red), is distributed uniformly, thereby confirming that no specific range of response is biased or disproportionately affecting the model. In summary, this plot substantiates the model assumptions, the reliability of the experimental data, and the appropriateness and statistical soundness of the developed factorial model for predicting particle size within the studied design space.

3.16.7. Predicted vs Actual Data for Particle Size

The comparison of the predicted and actual plots for particle size indicates a strong correlation between experimental and model-predicted values, thereby substantiating the high precision and dependability of the developed factorial model. The data points are observed to be concentrated along a 45-degree diagonal line, indicative of optimal prediction accuracy. This suggests that the model predictions align closely with the observed values (Fig. S10). The absence of significant deviation or scattering from this line suggests that there is minimal prediction error and no systematic bias in the model.

Furthermore, the uniform distribution of points across the entire particle size range (approximately 246 nm to 498 nm), as indicated by the color gradient, confirms that the model performs consistently well across both low and high response values. This strong correlation is also in agreement with the very high R^2 and predicted R^2 values obtained earlier, reinforcing the model's robustness and predictive capability. In summary, the empirical evidence corroborates the efficacy of the developed regression model in accurately predicting and optimizing particle size within the designated experimental domain.

3.16.8 Response 2- Pareto graph of Percent Drug Release

The Pareto chart of standardized effects offers a clear illustration of the relative significance and magnitude of the main and interaction effects on particle size. Factors A (concentration of soya lecithin), C (time), and B (temperature) demonstrate the highest t-values and intersect the reference significance line, indicating their statistical significance as contributors to the response (Fig. S11).

Among these factors, Factor A demonstrates the most significant positive effect, thereby confirming that increasing lecithin concentration results in a substantial increase in particle size, thus establishing it as the predominant factor. Conversely, factors B and C demonstrate adverse outcomes, suggesting that elevated temperatures and extended reaction times result in a substantial decrease in particle size, attributable to enhanced molecular interaction and augmented phytosome formation. The interaction terms AB, AC, and BC, along with any higher-order interactions, are positioned well below the significance threshold, demonstrating that their contributions are minimal and statistically insignificant. This finding indicates that the system is predominantly governed by individual factor effects rather than by combined interactions. In essence, the Pareto analysis substantiates the notion that the optimization of particle size is predominantly contingent on the independent regulation of lecithin concentration, temperature, and duration. Among these variables, lecithin concentration exerts the most substantial influence.

3.17. ANOVA for selected factorial model

3.17.1. Response 2: Percent Drug Release

The results of the analysis of variance (ANOVA) for the percentage of drug release clearly indicate that the developed factorial model is statistically significant ($F = 1506.67$, $p = 0.0197$), demonstrating that the selected formulation and process variables have a strong influence on drug release behavior, Table S15.

Among the primary effects, Factor A (concentration of soya lecithin) demonstrates the most significant contribution (Sum of Squares = 389.48, $F = 6010.56$, $p = 0.0082$), substantiating its role as the predominant factor influencing drug release, with increased lecithin concentration exhibiting a substantial reduction in drug release attributable to the formation of a more substantial lipid barrier. Factor C (time) also exhibited a highly significant effect ($F = 1938.45$, $p = 0.0145$), indicating that increasing reaction time enhances drug release by promoting complete phytosome formation and improved drug availability. In a similar vein, Factor B (temperature) exhibited a substantial positive impact ($F = 1089.00$, $p = 0.0193$), indicating that elevated temperatures promote enhanced drug–phospholipid interaction and augmented release. Conversely, the interaction terms AB, AC, and BC exhibited remarkably low F-values and high p-values (>0.05), suggesting that these interactions are statistically insignificant and do not significantly contribute to the variation in drug release. The remarkably minimal residual error (0.0648) substantiates the model's exceptional compatibility with minimal residual variability. The analysis demonstrates that percent drug release is predominantly governed by the individual effects of lecithin concentration, temperature, and time, with negligible interaction effects. This validates the robustness and predictive capability of the factorial design model.

3.17.2. Fit Statistics

The statistical parameters for percent drug release demonstrate that the developed model is highly precise, reliable, and robust. The standard deviation (0.2546) is remarkably low, suggesting minimal variation between experimental and predicted values, thereby demonstrating the model's exceptional precision, Table S16. The coefficient of variation (C.V. = 0.3097%), being far below 10%, confirms outstanding reproducibility and consistency of the experimental data.

The R^2 value (0.9999) indicates that 99.99% of the variability in drug release is explained by the model, signifying an almost perfect fit. This conclusion is further substantiated by the adjusted R^2 value of 0.9992, which approaches 1.0 and indicates a high degree of model fit, thereby confirming that the model is not overfitted and that all included terms are statistically significant. Additionally, the predicted R^2 (0.9929) is in excellent agreement with the adjusted R^2 (difference < 0.2), thereby demonstrating the model's strong predictive capability for new observations. The Adeq Precision value (116.8330), which is considerably higher than the requisite minimum of 4, signifies an exemplary signal-to-noise ratio and validates the model's capacity to adeptly navigate the design space. The statistical indicators demonstrate the model's remarkable precision, reproducibility, and suitability for optimization and prediction of percent drug release in phytosomal formulations.

3.17.3. Coefficients in Terms of Coded Factors

The regression coefficients, expressed in terms of coded factors for percent drug release, offer a quantitative understanding of the influence of each variable on the response. The intercept value (82.19) indicates the mean drug release at the midpoint levels of all factors. The primary outcomes indicate that factor A (concentration of soy lecithin) demonstrates a substantial negative coefficient of -6.98, signifying that an augmentation in lecithin concentration results in a considerable diminution in drug release, Table S17. This phenomenon is predominantly attributable to the formation of a more substantial phospholipid barrier, which impedes the diffusion of the drug.

In contrast, Factor B (temperature, +2.97) and Factor C (time, +3.96) exhibit positive coefficients, suggesting that increasing temperature and reaction time enhances drug release by improving drug-phospholipid interaction and ensuring complete phytosome formation. Notably, time exerts a slightly greater effect than temperature. The interaction terms AB (-0.0175), AC (+0.0950), and BC (-0.0825) have been found to have very small coefficient values, and their confidence intervals include zero. This indicates that these interactions are statistically insignificant and have negligible practical impact on drug release. Moreover, the VIF values of 1.000 for all factors confirm the absence of multi collinearity, thereby ensuring that the model estimates are stable and reliable. The comprehensive analysis reveals that percent drug release is predominantly influenced by the specific effects of lecithin concentration (negative influence) and process variables such as temperature and time (positive influence), with minimal contribution from interaction effects. This validates the model's robustness and interpretability.

3.17.3. Final Equation in Terms of Coded Factors

The final regression equation, expressed in terms of coded factors, offers a comprehensive mathematical representation of the influence of formulation and process variables on percent drug release. The intercept (82.19) is indicative of the mean drug release at the central levels of all factors. The primary outcomes indicate that factor A (concentration of soy lecithin) exhibits a substantial negative coefficient of -6.98.

Percent Drug Release = +82.19-6.98*A+2.97*B+3.96*C-0.0175*AB+0.0950* AC-0.0825*BC

This finding suggests that an augmentation in lecithin concentration results in a considerable diminution in drug release. This phenomenon is predominantly attributed to the formation of a more rigid and substantial phospholipid matrix, which impedes drug diffusion. In contrast, Factor B (temperature, +2.97) and Factor C (time, +3.96) show positive coefficients, demonstrating that increasing temperature and reaction time enhances drug release. This phenomenon is likely due to improved drug–phospholipid interaction, better solubilization, and more complete phytosome formation. Notably, time exerts a slightly stronger influence than temperature. The interaction terms AB (-0.0175), AC (+0.0950), and BC (-0.0825) have very small coefficients compared to the main effects, indicating that their contributions are negligible and that there is minimal interaction between variables. The equation as a whole confirms that percent drug release is predominantly governed by the individual effects of lecithin concentration (negative influence) and processing parameters such as temperature and time (positive influence).

3.17.4. Final Equation in Terms of Actual Factors

The final regression equation, expressed in terms of actual factors, provides a practical and quantitative understanding of how each formulation and process variable directly influences percent drug release. The intercept (68.29750) signifies the baseline drug release when all variables are at their zero level within the model context. The negative coefficient for concentration of soya lecithin (-0.145050) indicates that increasing lecithin concentration decreases drug release. This phenomenon can be attributed to the formation of a thicker and more rigid phospholipid matrix that restricts drug diffusion.

Percent Drug Release = +68.29750-0.145050*Concentration of Soya Lecithin+0.335250*Temperature+0.139083*Time-0.000035*Concentration of Soya Lecithin*Temperature+0.000063*Concentration of Soya Lecithin * Time-0.000275*Temperature *Time

Conversely, an increase in temperature (+0.335250) exhibited a pronounced positive effect, suggesting that elevated temperatures substantially augment drug release. This phenomenon can be attributed to enhanced molecular mobility and enhanced drug-phospholipid interaction. In a similar vein, the duration of processing (+0.139083) has been shown to exert a positive influence on the release of drugs. This suggests that an increase in processing time may promote more uniform phytosome formation and enhanced drug availability. However, the effect of processing duration on these outcomes is less pronounced in comparison to the effect of temperature. The interaction terms, including lecithin × temperature (-0.000035) and temperature × time (-0.000275), demonstrate negligible effects, suggesting a negligible interaction with a slight reduction in release when both variables increase simultaneously. Conversely, lecithin × time (+0.000063) exhibits a minimal positive contribution. The magnitudes of the interaction coefficients, when considered alongside the main effects, were found to be relatively small. This finding serves to corroborate the hypothesis that percent drug release is predominantly governed by individual factors, such as lecithin concentration (which exerts a negative influence) and temperature (which exerts a strong positive influence). The model can thus be reliably used for prediction and optimization of drug release within the studied design space.

3.17.5. Normal plot of Residuals for percent drug release

The standard plot of residuals for percent drug release demonstrates that the developed regression model satisfies the fundamental assumption of a normal distribution of residuals, which is essential for the validity of ANOVA and predictive modelling (Fig. S12). The data points are observed to align closely along a straight vertical line without noticeable curvature or systematic deviation, indicating that the residuals are randomly distributed and follow a normal pattern.

The absence of extreme outliers or points deviating significantly from the trend indicates the non-existence of experimental anomalies or influential data points. Furthermore, the distribution of residuals appears to be consistent across the range, thereby confirming the homoscedasticity (constant variance) of errors. The color gradient, representing the range of percent

drug release values (68.21% to 95.85%), is distributed evenly, indicating that the model performs uniformly across low and high response values without bias. In summary, the findings of this study corroborate the assumptions of normality and independence, thereby validating the model's statistical soundness, reliability, and suitability for precise prediction and optimization of percent drug release within the designated design space.

3.17.6. Predicted vs Actual data for percent drug release

The comparison of the predicted and actual plots for percent drug release demonstrates a strong correlation between experimental and model-predicted values, thereby confirming the high accuracy and robustness of the developed factorial model. All data points exhibited a close alignment along the 45-degree diagonal line, signifying perfect agreement between predicted and actual responses (Fig. S13).

This finding suggests that the model predictions are highly precise, with minimal deviation or residual error. The uniform distribution of points across the entire response range (approximately 68% to 96%), as indicated by the color gradient, suggests that the model performs consistently well for both low and high drug release values without any systematic bias. The absence of any discernible scattering or clustering away from the line is indicative of the absence of both under prediction and over prediction trends. This robust agreement aligns with the previously observed high R^2, adjusted R^2, and predicted R^2 values, thereby further substantiating the model's predictive capacity. In sum, the empirical evidence corroborates the efficacy of the developed regression model, validating its reliability and suitability for precise prediction and optimization of percent drug release within the delineated experimental design space.

3. 18. Optimization

The optimization study, based on a factorial design, clearly demonstrates that the simultaneous adjustment of formulation and process variables is critical for achieving the desired response, i.e., minimum particle size and maximum percent drug release [18-19].

The negligible contribution of interaction terms further simplifies the optimization process, indicating that factors can be adjusted independently without significant combined effects. The high desirability value (close to 1) confirms that the selected conditions provide an excellent compromise between all responses. The optimization results demonstrate the robustness of the factorial design and confirm the efficacy of the developed model in predicting and obtaining an optimized phytosomal formulation with superior physicochemical and release characteristics.

3.18.1. Criteria for Optimization of Response Particle size

The numerical optimization plot for particle size provides a clear illustration of the desirability function applied to achieve minimum particle size within the defined range (246.14-498.06 nm). The objective designated as "minimize" signifies that achieving lower particle size values is preferable, as illustrated by the descending desirability ramp. The left side of the graph (approximately 246.14 nm) corresponds to the region of maximum desirability, indicating optimal formulation conditions, while the right side (approximately 498.06 nm) represents the least desirable outcome (Fig. S14).

The location of the selected point in proximity to the lower end indicates that the optimization algorithm has identified conditions that favor smaller particle size, which is consistent with the optimized batch (B7). The equal weighting (weight = 1) and high importance setting (+++) indicate that particle size was regarded as a critical response during optimization. This graphical representation substantiates the hypothesis that a reduction in lecithin concentration, coupled with an augmentation in temperature and duration, results in a shift of the response toward the most optimal region. The optimization plot provides a comprehensive validation of the efficacy of the selected formulation conditions in achieving the targeted objective of reducing particle size. Furthermore, the model's capacity to reliably guide formulation optimization within the defined design space is substantiated.

3.18.2. Criteria for Optimization of Response Cumulative percent drug release

The numerical optimization plot for percent drug release provides a clear illustration of the application of the desirability function to achieve the objective of maximizing drug release within the specified range (68.21%-95.85%). The upward slope of the desirability ramp indicates that higher values of percent drug release are more desirable, with the maximum desirability achieved near the upper limit (95.85%),

Corresponding to the optimized formulation, the selected point, located in close proximity to the upper boundary, substantiates the efficacy of the optimization process in identifying formulation conditions that promote maximal drug release. This finding corresponds with the optimized batch (B7). The equal weighting (weight = 1) and high importance setting (+++) indicate that drug release was treated as a critical response during optimization. This plot also reflects the influence of formulation variables, where lower lecithin concentration and higher temperature and time contribute to enhanced drug release (Fig. S15). The smooth and continuous desirability curve indicates a stable and predictable response behaviour across the design space.

3.18.3. Solutions

The numerical optimization results, which present 57 possible solutions, clearly demonstrate the robustness and flexibility of the factorial design in achieving the desired goals of minimum particle size and maximum percent drug release. Among these, Solution 1 (selected) demonstrates the highest desirability value (1.000), indicating an ideal balance between both responses, with optimized conditions of approximately 100.6 mg lecithin, 69.99°C temperature, and 150 min time, yielding a particle size of 245.67 nm and drug release of 95.85%, Table S18.

A critical observation across the top-ranked solutions (1-10) is that they are tightly clustered within a narrow range of factor levels, particularly low lecithin concentration (~100 mg), high temperature (~70°C), and maximum time (~150 min), confirming that this region represents the true optimal design space. As the solution number increases, a gradual shift is observed either an increase in lecithin concentration or a decrease in temperature and time. This shift leads to an increase in particle size and a decrease in drug release, which in turn lowers the desirability value. The proximity of the desirability values to 1 for multiple solutions suggests that the optimization is not constrained to a single point but rather persists within a stable optimal region, thereby providing formulation flexibility. However, beyond this region (solutions >30), a significant decline in desirability is observed due to unfavorable factor combinations, particularly increased lecithin or reduced temperature.

3.18.4. Effect of Concentration of Soya Lecithin and Temperature on Particle Size

The 3D surface plot provides a visual representation of the combined effect of concentration of soya lecithin (Factor A) and temperature (Factor B) on particle size, while keeping time (Factor C) constant at approximately 150 minutes. This provides a clear visualization of the interaction and trend behavior within the design space.

The surface of the samples exhibited a gradual increase in particle size with increasing lecithin concentration, as evidenced by the transition from blue (lower particle size, 246.14 nm) to green/yellow regions (higher particle size, 498.06 nm). This observation confirms that higher lipid content leads to the formation of larger vesicular structures due to increased bilayer thickness and aggregation tendency (Fig. S16). Conversely, an increase in temperature results in a slight reduction in particle size, evident from the downward slope along the temperature axis. This phenomenon can be attributed to enhanced molecular mobility and improved dispersion of lipid molecules at higher temperatures. The contour lines at the base further substantiate this trend, demonstrating a consistent gradient without abrupt curvature, thereby indicating a predominantly linear relationship with minimal interaction between factors A and B. This finding aligns with the statistical insignificance of interaction terms observed in ANOVA. The relatively smooth and planar surface suggests the absence of strong synergistic or antagonistic effects between lecithin concentration and temperature. The plot overall confirms that minimum particle size is achieved at low lecithin concentration and higher temperature. This validates the optimization results and demonstrates that these two factors independently influence particle size within the studied experimental domain.

3.18.5. Effect of Concentration of Soya Lecithin and Time on Particle Size

The 3D surface plot (Fig. S17) illustrates the combined influence of concentration of soya lecithin (Factor A) and time (Factor C) on particle size, while maintaining temperature (Factor B) constant at 69.991 (Appx 70) °C. This method enables the visualization of their interaction and individual contributions. The surface of the sample displays a marked increase in the size of the particles with an increase in lecithin concentration.

This observation is supported by a color transition from blue (246.14 nm) at lower concentrations (100 mg) to green/yellow regions (498.06nm) at higher concentrations (200 mg). This transition indicates that an increase in lipid content promotes the formation of larger vesicles due to increased bilayer thickness and potential aggregation. Conversely, an increase in processing time results in a modest reduction in particle size, as evidenced by the slight downward trend along the time axis. This

phenomenon can be ascribed to enhanced homogenization, enhanced drug-lipid interaction, and the stabilization of smaller particles over an extended period of processing. The contour lines at the base are relatively straight and parallel, suggesting a predominantly linear relationship with minimal interaction between lecithin concentration and time. This finding is consistent with the statistically insignificant AC interaction term observed in the model. The absence of curvature or strong synergistic effects is indicated by the smooth planar nature of the surface. The findings of this study demonstrate that the minimum particle size is attained at low lecithin concentrations and elevated processing times. These results corroborate the outcomes of the optimization process and underscore the pivotal role of lecithin concentration in influencing particle size reduction. The analysis further substantiates that processing time contributes as a secondary yet advantageous parameter in this process.

3.18.6. Effect of Temperature and Time on Particle Size

The 3D surface plot (Fig. S18) offers a representation of the combined effect of temperature (Factor B) and time (Factor C) on particle size, while maintaining a constant concentration of soya lecithin (Factor A) at 100.6 mg. This approach enables a targeted evaluation of the process variables.

The surface displays a gradual decrease in particle size with increasing temperature and time, as evidenced by the transition from green/yellow regions (~350-400 nm) at lower temperatures and shorter times to blue regions (~250-300 nm) at higher temperatures and longer times. This trend lends further credence to the hypothesis that elevated temperatures enhance molecular mobility and improve drug-phospholipid interaction. In addition, the findings suggest that an extended processing time promotes complete phytosome formation and better size uniformity, resulting in smaller particles. The surface appears to be smooth and nearly planar, and the contour lines at the base are relatively straight and parallel, indicating a predominantly linear relationship with minimal interaction between temperature and time. This finding aligns with the statistically insignificant BC interaction term observed in ANOVA. The absence of curvature or substantial synergistic effects indicates that both factors independently contribute to particle size reduction. The findings of this study demonstrate that the optimal (minimum) particle size is achieved at higher temperatures and longer times. These results reinforce the optimization results and confirm the beneficial role of these process parameters in improving phytosomal characteristics.

3.18.7. Contour plot of Concentration of Soya Lecithin and Temperature on Particle Size

The contour plot (Fig. S19) illustrates the combined effect of concentration of soya lecithin (Factor A) and temperature (Factor B) on particle size, while keeping time (Factor C) constant at 150 minutes, enabling clear visualization of response variation within the design space.

The color gradient transitions from blue (lower particle size 246.14 nm) at low lecithin concentration and high temperature to green/yellow (higher particle size 498.06 nm) at higher lecithin concentration and lower temperature. This indicates that particle size increases significantly with increasing lecithin concentration and decreases with increasing temperature. The contour lines exhibit a high degree of linearity and parallelism, suggesting a minimal interaction between factors A and B. This finding is consistent with the statistically insignificant AB interaction term observed in the analysis of variance (ANOVA). The diagonal orientation of contour lines further corroborates the hypothesis that both factors independently influence the response, with lecithin concentration exhibiting a stronger effect compared to temperature. The region of minimum particle size is evidently situated at low lecithin concentrations (100 mg) and elevated temperatures (70°C), while the maximum particle size is attained at high lecithin concentrations (200 mg) and low temperatures (50°C). The plot substantiates the hypothesis that lecithin concentration is the predominant factor controlling particle size, while temperature functions as a supportive factor in reducing particle size. The absence of curvature confirms the adequacy of the linear factorial model within the studied range.

3.18.8. Contour plot of Concentration of Soya Lecithin and Time on Particle Size

The contour plot (Fig. S20) illustrates the combined effect of concentration of soya lecithin (Factor A) and time (Factor C) on particle size, while keeping temperature (Factor B) constant at approximately 70°C. This provides insight into how formulation and process duration interact within the design space.

The color gradient clearly demonstrates that particle size increases with increasing lecithin concentration, transitioning from blue (246.14nm) at lower concentrations (100 mg) to green/yellow regions (498.06 nm) at higher concentrations (200 mg). This confirms the dominant role of lecithin in increasing vesicle size due to enhanced lipid bilayer thickness and aggregation.

Conversely, an increase in processing time results in a gradual decrease in particle size, as evidenced by the shift toward cooler colors along the time axis. This phenomenon can be attributed to enhanced homogenization, enhanced drug-phospholipid interaction, and stabilization of smaller vesicles over extended processing. The contour lines are straight, parallel, and diagonally oriented, indicating a linear relationship with minimal interaction between lecithin concentration and time, consistent with the statistically insignificant AC interaction term observed in the model. The region of minimum particle size is located at low lecithin concentration (100 mg) and higher time (150 min), whereas maximum particle size occurs at high lecithin concentration and lower processing time. In essence, the experimental findings substantiate the notion that lecithin concentration exerts a predominant influence on the observed outcomes, with time serving a subsidiary function in the reduction of particle size. The absence of curvature corroborates the sufficiency of the linear factorial model within the designated experimental range.

3.18.9. Contour plot of Temperature and Time on Particle Size

The contour plot (Fig. S21) illustrates the combined influence of temperature (Factor B) and time (Factor C) on particle size, while maintaining a constant concentration of soya lecithin (Factor A) at 100.6 mg. This method allows for the isolation of the effect of process variables.

The color gradient displays a discernible transition from yellow/green regions (higher particle size 498.06 nm) at lower temperature and shorter time to blue regions (lower particle size 246.14 nm) at higher temperature and longer time, suggesting that particle size diminishes as both temperature and time increase. This phenomenon can be attributed to enhanced molecular mobility at elevated temperatures and improved drug-phospholipid interaction and stabilization over extended processing times, leading to the formation of smaller and more uniform phytosomal vesicles. The contour lines exhibit a smooth and slightly curved pattern, largely parallel to one another, suggesting a predominantly linear relationship with a mild interaction effect between temperature and time, although this effect is not statistically significant. The region of minimum particle size is evidently situated at elevated temperatures (70°C) and protracted times (150 min), while the maximum particle size is discerned at reduced temperatures (50°C) and abbreviated times (90 min). The findings of this study demonstrate that both temperature and time independently contribute to particle size reduction, with temperature exhibiting a slightly stronger influence. These results support the optimization findings that higher process conditions favor improved phytosomal characteristics.

3.18.10. Effect of Concentration of Soya Lecithin and Temperature on Percent Drug Release (%)

The 3D surface plot (Fig. S22) illustrates the combined effect of concentration of soya lecithin (Factor A) and temperature (Factor B) on percent drug release, while keeping time (Factor C) constant at approximately 150 min. This method highlights both formulation and process influences on drug release behaviour. The surface displays a discernible trend, wherein the percentage of drug release declines with rising lecithin concentrations.

This transition is evidenced by the shift from red/orange regions (95.86%) at lower lecithin levels (100 mg) to green regions (68.21%) at higher concentrations (200 mg). This finding indicates that higher lecithin concentrations form a thicker phospholipid matrix, which restricts drug diffusion and slows release. Conversely, an increase in temperature has been shown to result in enhanced drug release, as evidenced by the upward slope along the temperature axis. This phenomenon can be attributed to improved molecular mobility, enhanced drug–lipid interaction, and increased permeability of the phytosomal system. The contour lines at the base are relatively straight and parallel, indicating a predominantly linear relationship with minimal interaction between lecithin concentration and temperature. This finding is consistent with the statistically insignificant AB interaction term observed in ANOVA. The absence of strong synergistic effects is indicated by the smooth planar surface. The region of maximum drug release is observed at low lecithin concentration (100 mg) and high temperature (70°C), while minimum release occurs at high lecithin and low temperature. The plot substantiates the hypothesis that lecithin concentration exerts a dominant negative effect on drug release, while temperature demonstrates a supportive positive role. These observations validate the optimization results and demonstrate predictable behaviour within the studied design space.

3.18.11. Effect of Concentration of Soya Lecithin and Time on Percent Drug Release (%)

The 3D surface plot (Fig. S23) illustrates the combined effect of concentration of soya lecithin (Factor A) and time (Factor C) on percent drug release, while maintaining temperature (Factor B) constant at approximately 70°C. This method allows for the isolation of the influence of formulation and processing duration.

The surface clearly demonstrates a decrease in percent drug release with increasing lecithin concentration, as indicated by the transition from red/orange regions (95.85%) at lower concentrations (100 mg) to green/blue regions (68.21%) at higher concentrations (200 mg). This confirms that higher lipid content forms a thicker phospholipid matrix, which restricts drug diffusion. Conversely, an increase in processing time has been shown to result in enhanced drug release, as demonstrated by the rising trend along the time axis. This phenomenon can be attributed to improved drug-phospholipid interaction, enhanced solubilization, and more complete phytosome formation during extended processing. The contour lines at the base are straight and parallel, indicating a linear relationship with minimal interaction between lecithin concentration and time. This finding aligns with the statistically insignificant AC interaction term observed in ANOVA. The absence of significant synergistic or antagonistic effects is indicated by the smooth planar surface. The region of maximum drug release is observed at low lecithin concentrations (100 mg) and higher times (150 min), while minimum release occurs at high lecithin concentrations and shorter times. The study's findings indicate that the concentration of lecithin exerts a negative influence on drug release, while the duration of processing has a positive effect on the release process. These results support the hypothesis that lower lecithin concentrations and extended processing times lead to enhanced drug release performance.

3.18.12. Effect of Temperature and Time on Percent Drug Release (%)

The 3D surface plot (Fig. S24) provides a representation of the combined influence of temperature (Factor B) and time (Factor C) on percent drug release, while maintaining a constant concentration of soya lecithin (Factor A) at approximately 100.6 mg. This approach serves to accentuate the effect of process variables on release behaviour. The surface displays a discernible increasing trend in percent drug release with rising temperature and duration, as evidenced by the transition from green regions (68.21%) at lower temperatures and shorter times to orange/red regions (98.85%) at higher temperatures and longer times. This phenomenon suggests that elevated temperatures enhance molecular mobility, thereby improving drug-phospholipid interaction. Furthermore, an extended processing time ensures complete phytosome formation, leading to enhanced drug availability. Collectively, these factors result in enhanced drug release. The surface appears to be smooth and nearly planar, and the contour lines at the base are straight and parallel, indicating a predominantly linear relationship with minimal interaction between temperature and time. This finding is consistent with the statistically insignificant BC interaction term observed in ANOVA. The absence of curvature or substantial synergistic effects indicates that both factors independently contribute to enhancing drug release.

The region of maximum drug release is clearly observed at higher temperatures (70°C) and longer times (150 minutes), while minimum release occurs at lower temperatures and shorter times. The findings of this study demonstrate that both temperature and time have a positive influence on drug release. These results support the hypothesis that higher process conditions are conducive to achieving maximum drug release in phytosomal formulations.

3.18.13. Contour plot of Concentration of Soya Lecithin and Temperature on Percent Drug Release (%)

The contour plot (Fig. S25) illustrates the combined effect of concentration of soya lecithin (Factor A) and temperature (Factor B) on percent drug release, while keeping time (Factor C) constant at approximately 150 minutes. This clearly depicts how formulation and thermal conditions influence drug release behavior. The color gradient transitions from red/orange regions (95.85% drug release) at low lecithin concentration (100 mg) and high temperature (70°C) to green/blue regions (68.21%) at higher lecithin concentration (200 mg) and lower temperature (50°C). These results indicate that drug release decreases significantly with increasing lecithin concentration and increases with rising temperature. This finding indicates that higher lecithin concentrations form a thicker phospholipid matrix, thereby restricting drug diffusion. Conversely, elevated temperatures enhance molecular mobility and drug-lipid interaction, facilitating enhanced release. The contour lines are straight, parallel, and diagonally oriented, indicating a linear relationship with minimal interaction between lecithin concentration and temperature, consistent with the statistically insignificant AB interaction term observed in ANOVA.

The presence of a diagonal pattern indicates that both factors independently influence the response, with lecithin concentration exhibiting a more pronounced negative effect compared to the positive effect of temperature. The region of maximum drug release is evidently situated at low lecithin concentrations and elevated temperatures, while minimum release is observed at high lecithin concentrations and low temperatures. In summary, the plot substantiates the notion that lecithin concentration exerts a predominant influence on the regulation of drug release, exhibiting an inverse relationship with temperature. This observation aligns with the optimized results and validates the efficacy of the linear factorial model in depicting the underlying mechanisms.

3.18.14. Contour plot of Concentration of Soya Lecithin and Time on Percent Drug Release (%)

The contour plot (Fig. S26) illustrates the combined effect of concentration of soya lecithin (Factor A) and time (Factor C) on percent drug release, while keeping temperature (Factor B) constant at approximately 70°C. This method emphasizes the influence of formulation and processing duration. The color gradient displays a discernible transition from red/orange regions (95.85% drug release) at lower lecithin concentrations (100 mg) and extended times (150 min) to green/blue regions (68.21%) at higher lecithin concentrations (200 mg) and abbreviated times (90 min). This observation signifies that drug release diminishes with increasing lecithin concentration and escalates with prolonged duration. This phenomenon can be attributed to the formation of a thicker phospholipid matrix at higher lecithin levels, which restricts drug diffusion. Conversely, prolonged processing time enhances drug-phospholipid interaction, improves solubilization, and facilitates more complete phytosome formation, leading to higher drug release. The contour lines are straight, parallel, and diagonally oriented, suggesting a linear relationship with minimal interaction between lecithin concentration and time, consistent with the statistically insignificant AC interaction term observed in ANOVA.

The diagonal orientation indicates that both factors independently influence the response, with lecithin concentration exerting a stronger negative effect compared to the positive effect of time. The region of maximum drug release is observed at low lecithin concentrations and higher processing times, while minimum release occurs at high lecithin concentrations and shorter times. In summary, the findings of the present study demonstrate that the concentration of lecithin functions as the primary factor that exerts an inverse influence on the process of drug release. Concurrently, the temporal factor has been shown to promote the enhancement of release. These observations serve to provide substantiation for the optimization results and to validate the linear factorial model within the designated design space.

3.18.15. Contour plot of Temperature and Time on Percent Drug Release (%)

The contour plot (Fig. S27) illustrates the combined effect of temperature (Factor B) and time (Factor C) on percent drug release, while keeping the concentration of soya lecithin (Factor A) constant at 100.6 mg. This method isolates the influence of process variables. The color gradient transitions from green regions (68.21 % drug release) at lower temperatures (50°C) and shorter times (90 min) to yellow/orange/red regions (95.85 %) at higher temperatures (70°C) and longer times (150 min). This indicates that drug release increases with both temperature and time. This phenomenon can be attributed to enhance molecular mobility and improved drug–phospholipid interaction at elevated temperatures, along with more complete phytosome formation and better drug availability at longer processing times. The contour lines are straight, parallel, and diagonally oriented, suggesting a linear relationship with minimal interaction between temperature and time. This finding is consistent with the statistically insignificant BC interaction term observed in ANOVA.

The diagonal orientation indicates that both factors independently contribute to the increase in drug release, with temperature showing a slightly stronger influence than time. The region of maximum drug release is clearly observed at higher temperatures and longer times, while minimum release occurs at lower temperatures and shorter times. The findings of this study demonstrate that both temperature and time have a positive influence on drug release. These results support the optimization findings and validate the suitability of the linear factorial model within the studied design space.

The optimization study, which was carried out using Design-Expert software, identified an optimized formulation with a concentration of soya lecithin of 100.614 mg, a temperature of 69.991°C, and a duration of 149.999 minutes. This optimized formulation yielded a particle size of 245.671 nm and a percent cumulative drug release of 95.853%, illustrated in Table S19.

This optimized solution achieved a desirability value of 1.000, indicating an ideal balance between the targeted responses, namely minimization of particle size and maximization of drug release. The findings unequivocally substantiate that a

diminished lecithin concentration, concomitant with elevated temperatures and protracted processing times, is instrumental in attaining optimal phytosomal characteristics. The reduction in particle size under these conditions can be attributed to enhanced molecular dispersion and efficient phytosome formation. The enhanced drug release is attributable to a reduced lipid barrier thickness and increased drug availability. The optimized formulation falls within the predicted design space and aligns closely with the experimental trends observed in factorial analysis, thereby confirming the validity and predictive capability of the developed model. In summary, the optimized batch under consideration constitutes the most favourable formulation condition, providing a stable, efficient, and high-performance phytosomal delivery system suitable for further development and evaluation.

3.19. Optimized Batch Final formula

The optimized phytosomal formulation was developed using Asiatic acid and Bacopasaponinin c, Table S20, with the final composition obtained through numerical optimization. The formulation consists of 50 mg of each extract, combined with 100.614 mg of soy lecithin, processed at a temperature of approximately 70°C for 150 minutes, using dichloromethane (40 ml) and n-hexane (10 ml) as solvents. The employment of dichloromethane and n-hexane facilitates the effective evaporation and precipitation of the phytosomal complex. In summary, the optimized formulation under consideration exhibits an optimal balance between formulation and process variables. This balanced approach has been demonstrated to enhance physicochemical properties and drug release performance. The outcomes substantiate the dependability of the experimental design and substantiate the optimized batch as a promising phytosomal delivery system for enhanced bioavailability and therapeutic efficacy.

3.19.1. Evaluation of Optimized Batch

The optimized phytosomal Table S22, formulation had a high drug content (94.86%) and high entrapment efficiency (90.64%), indicating that the phytoconstituents were effectively incorporated into the vesicular system. The formulation had a nanosized particle diameter of 236.75 nm and a zeta potential of -35.23 mV, indicating good colloidal stability and uniform distribution. Furthermore, the optimized batch had a remarkable in-vitro drug release of 99.17%, indicating its potential for increased drug delivery and clinical efficacy.

3.20. Optimized Batch

3.20.1. Particle Size

The optimized phytosomal batch had a mean particle size (Fig. 2) (Z-average) of 236.75 nm and a PDI of 0.272, indicating a fairly consistent and narrow particle size distribution. The intensity distribution curve revealed a single conspicuous peak with 100% intensity, indicating that the vesicular formulation was homogeneous and did not exhibit considerable aggregation. Also, the high intercept value (0.938) and good result quality indicated that the optimized nano-sized phytosomal system was reliable and stable.

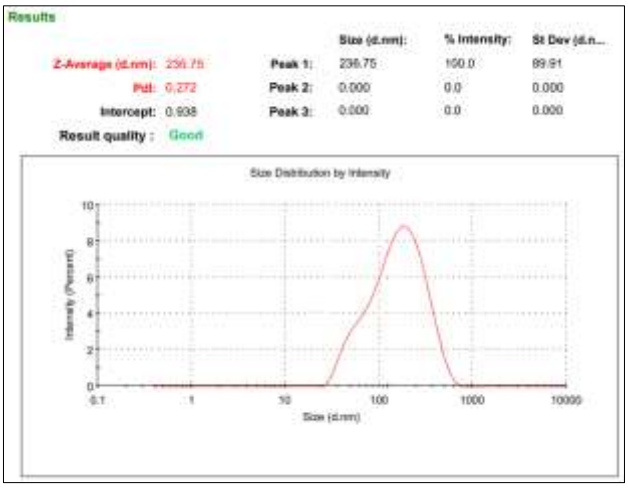


Fig. 2. Particle size plot of optimized batch

3.20.2. Zeta Potential

The optimized phytosomal formulation (Fig. 3) showed a zeta potential of -35.23 mV, indicating enough surface charge on the vesicles. The high negative zeta potential value indicated significant electrostatic repulsion between particles, which helps to increase physical stability and prevent aggregation. The single sharp peak with 100% area distribution and a modest zeta deviation (3.80 mV) verified the optimized batch's homogeneity and stability.

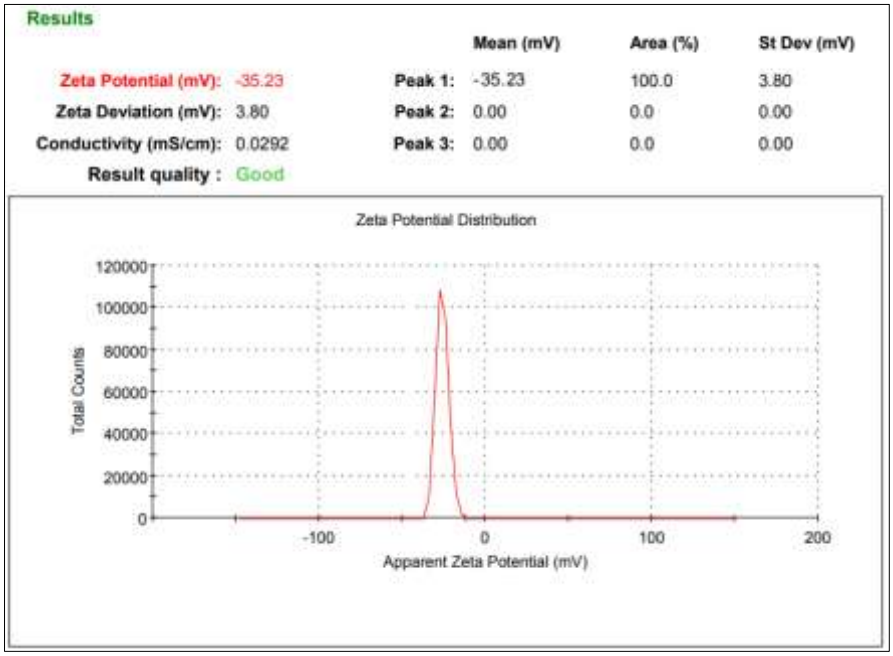


Fig. 3. Zeta potential plot of optimized batch

3.20.3. In-vitro release

The in vitro drug release profile of the optimized phytosomal (Table 1 and Fig. 4) batch showed an initial burst release, with approximately half of the drug released within the first two hours, followed by a controlled and continuous release pattern. The formulation produced 99-100% cumulative drug release over 24 hours, showing that the encapsulated phytoconstituents release efficiently. This biphasic release profile suggests that the optimized formulation may provide both an immediate therapeutic response and prolonged drug delivery, thereby increasing therapeutic efficacy and maintaining long-term pharmacological action.

Table 1 *In-vitro* release of optimize batch

Time (Hrs)	Optimized Batch
0	0
1	29.12 ± 1.5
2	45.84 ± 1.6
4	56.73 ± 1.8
6	76.44 ± 1.2
8	89.31 ± 1.4
12	94.76 ± 1.3
24	99.17 ± 1.5

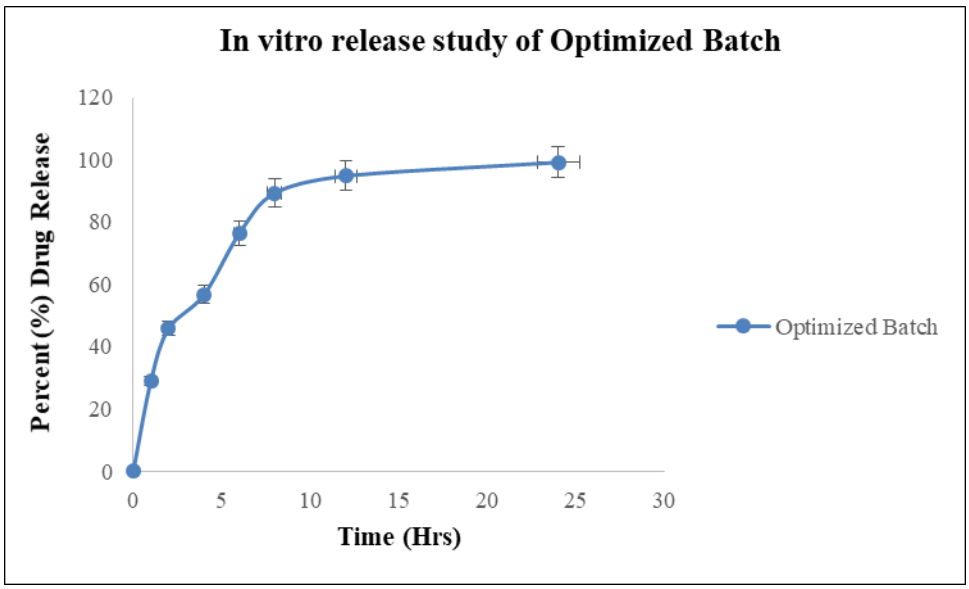


Fig. 4. Percent drug release profile of Optimized batch

3.20.4. DSC of Bacopasaponin C

The differential scanning calorimetry (DSC) thermogram of bacopasaponin c shows a sharp, distinct endothermic peak at around 202.5°C, which indicates the compound's thermal behaviour. The presence of a well-defined peak suggests that bacopasaponin c exists in a crystalline state, since amorphous materials typically exhibit broad or diffuse transitions rather than sharp peaks. The peak's height (18.7565 mW) and area (1426.415 mJ) reflect the energy absorbed during the phase transition, which corresponds to the compound's melting. The calculated enthalpy change ($\Delta H \approx 356.60$ J/g) confirms the presence of a strong crystalline lattice that requires a significant amount of energy to disrupt. The absence of multiple peaks indicates the purity of the sample, as the presence of additional peaks would suggest polymorphism or impurities. The sharp and narrow nature of the peak also supports a uniform distribution of crystal sizes (Fig. 5).

The DSC analysis confirms that bacopasaponin is a thermally stable, crystalline phytoconstituent, which is advantageous for formulation development. This thermal behaviour is important for designing phytosomal systems as it provides information on drug excipient compatibility and processing temperature limits, thereby ensuring stability during formulation and storage.

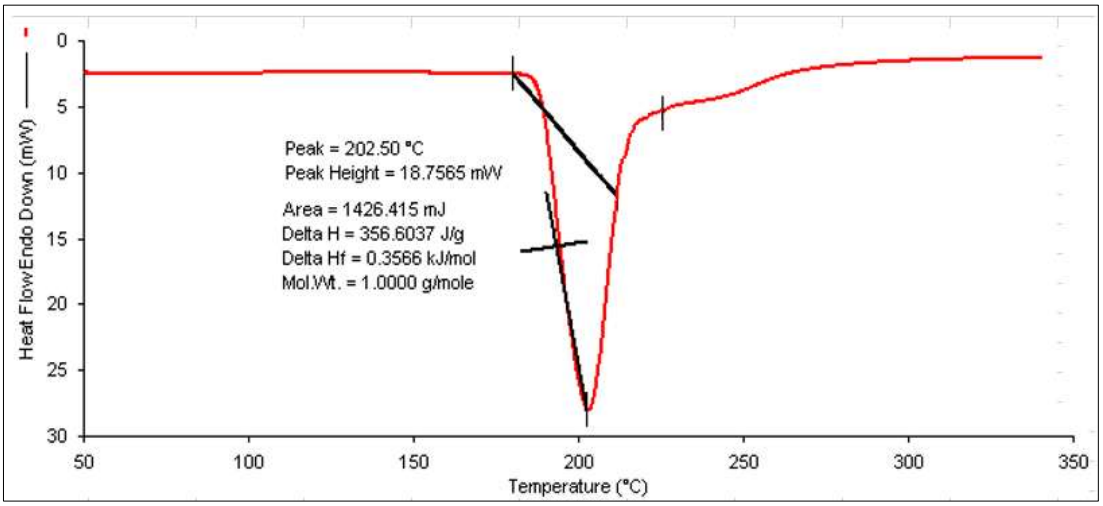


Fig. 5. DSC Thermogram of Bacopasaponin C

3.20.5. DSC of Asiatic acid

The differential scanning calorimetry (DSC) thermogram of asiatic acid shows a clear endothermic peak at 159.52 °C, which is its melting point. The sharp, well-defined nature of this peak confirms that Asiatic acid predominantly exists in crystalline form, indicating an ordered molecular arrangement. The peak's height (17.3648 mW) and area (1379.791 mJ) represent the energy absorbed during the melting process and reflect the strength of the interactions between molecules within the crystal lattice. The calculated enthalpy change (ΔH ≈ 319.95 J/g) suggests that a considerable amount of energy is required to disrupt the crystalline structure, which further supports its stable solid-state nature. The thermogram also (Fig. 6) shows a slight shoulder or secondary transition near the main peak, which may indicate minor polymorphic behaviour or the presence of trace impurities. However, the dominance of a single sharp peak suggests that the compound is largely pure. Additionally, the absence of any significant thermal events at lower temperatures indicates good thermal stability prior to melting, which is advantageous for formulation processes involving moderate heating. DSC analysis confirms that Asiatic acid is a crystalline and thermally stable phytoconstituent.

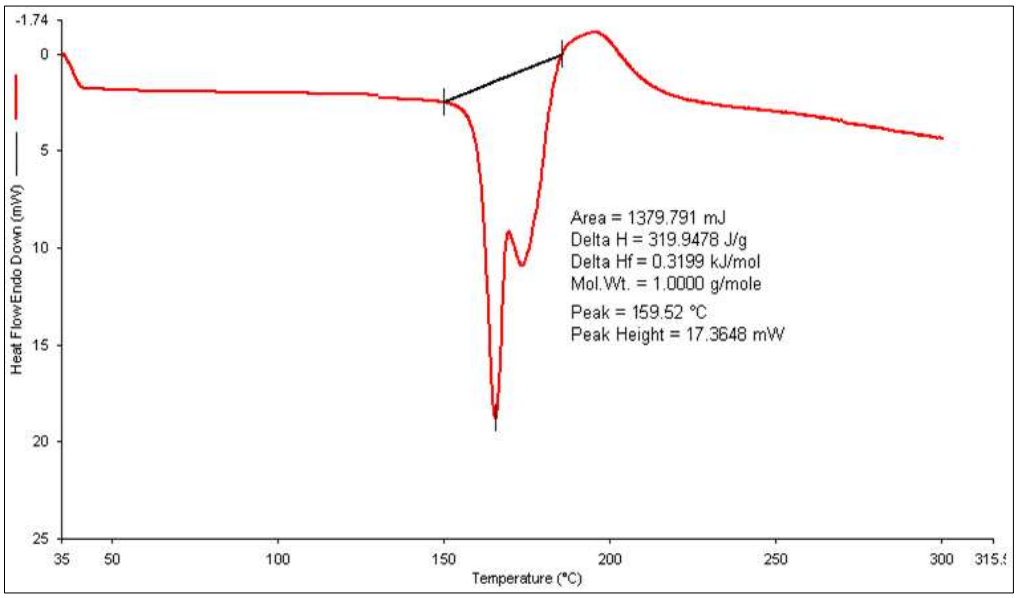


Fig. 6. DSC Thermogram for Asiatic acid

3.20.6. DSC of Phytosomal Formulation

The differential scanning calorimetry (DSC) thermogram (Fig. 7) of the optimised phytosomal formulation showed significant changes in thermal behaviour compared to the pure phytoconstituents (asiatic acid and bacopasaponin c). The sharp endothermic peaks characteristic of the individual components, which were previously observed at ~159.5°C and ~202.5°C, were found to be either shifted, broadened or completely diminished in the optimised formulation. These changes indicate the successful formation of a phytosome complex between the phytoconstituents and soya lecithin. The absence or reduction in intensity of the drug-specific melting peaks suggests a loss of crystallinity and conversion into a more amorphous or molecularly dispersed state within the phospholipid matrix. This transformation is attributed to strong interactions between the drug and phospholipids, such as hydrogen bonding and van der Waals forces, which lead to the encapsulation or complexation of the active constituents. The broad endothermic region observed in the thermogram corresponds to the thermal behaviour of the lipid matrix, confirming the incorporation of the drug into the lecithin bilayer system. Furthermore, the reduction in enthalpy values (ΔH) compared to pure compounds indicates decreased lattice energy, which supports the hypothesis of reduced crystallinity. The absence of additional unexpected peaks confirms the compatibility of the drug with the excipients, with no evidence of chemical degradation or interaction leading to instability. DSC analysis confirms the formation of a stable phytosomal complex characterised by reduced crystallinity, improved molecular dispersion and enhanced thermal compatibility. These findings strongly suggest that the optimized phytosomal system has improved solubility, bioavailability and formulation stability.

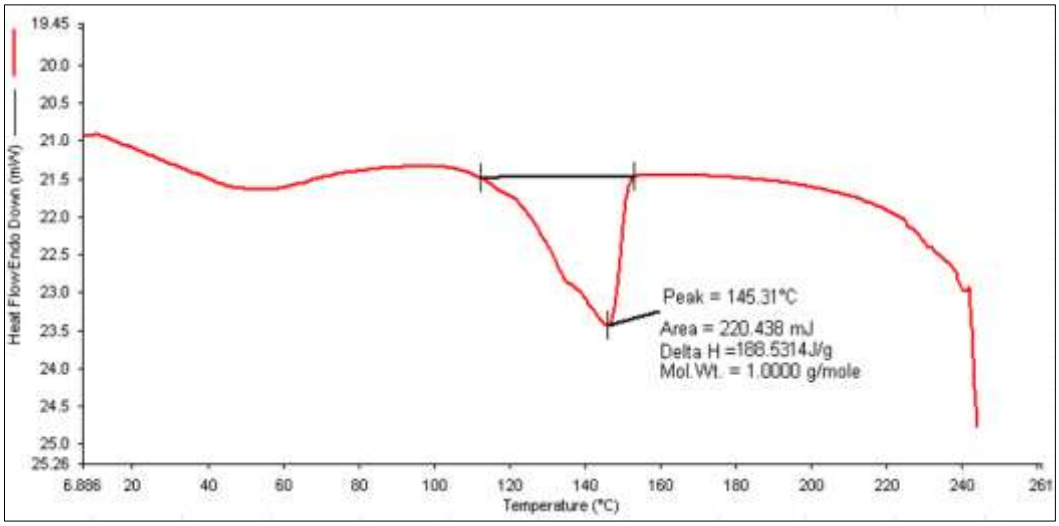


Fig. 7. DSC Thermogram of optimized phytosomal formulation

3.20.7. SEM Analysis

Scanning electron microscopy (SEM) (Fig. 8) analysis of the optimised phytosomal formulation revealed the morphological characteristics and surface topology of the prepared vesicular system. The SEM micrographs showed that the phytosomes were predominantly spherical or near-spherical in shape, with a smooth, uniform surface, indicating the successful formation of lipid-based vesicular structures. The particles appeared well-dispersed with minimal aggregation, suggesting effective stabilisation by soya lecithin and adequate processing conditions. The observed particle morphology corroborates the particle size data obtained via dynamic light scattering, confirming the formation of nano-sized vesicles with a narrow size distribution. The absence of irregular or crystalline structures in the micrographs suggests that the phytoconstituents (asiatic acid and Bacopasaponin C) have been successfully incorporated into the phospholipid matrix rather than existing as a free crystalline drug. This corroborates the DSC findings of reduced crystallinity. The smooth surface of the phytosomes also suggests a uniform coating and proper lipid bilayer formation, which is essential for improved drug entrapment and controlled release. The lack of surface cracks or pores indicates the formulation's good structural integrity and stability. SEM analysis confirms that the optimised phytosomal formulation possesses the desirable morphological characteristics of a spherical shape, a smooth surface and a uniform distribution.

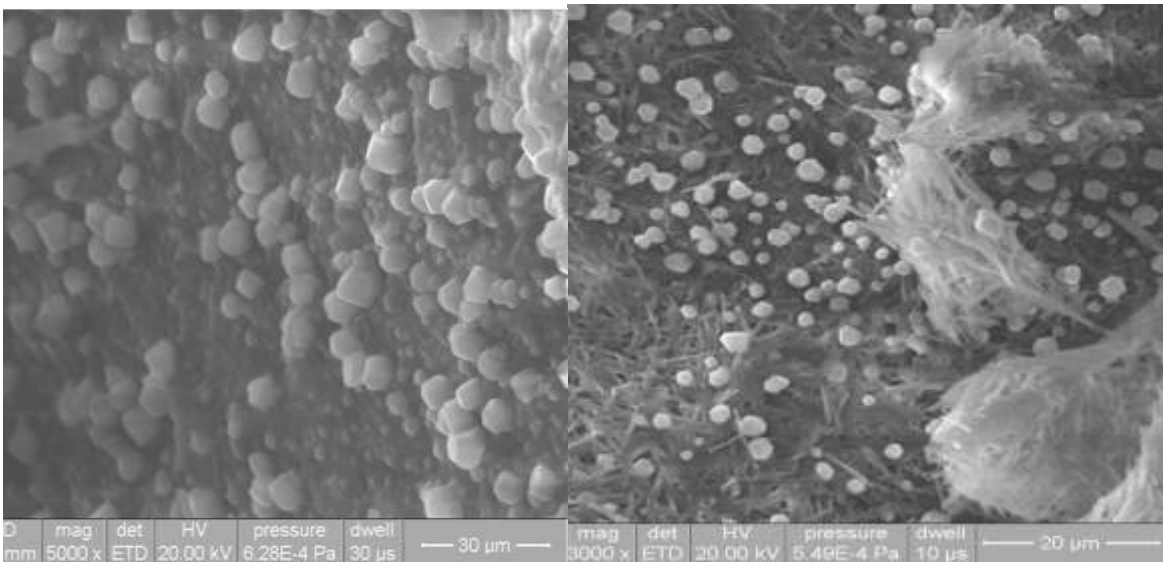


Fig. 8. SEM images of optimized Phytosomal Formulation

Natural Resources for Human Health
eISSN: 2583-1194

3.21. XRD Analysis

3.21.1. XRD of Bacopasaponin C

The XRD pattern of bacopasaponin c (Table 2 and Fig. 9) showed clear diffraction peaks at 2θ values of 15.2°, 22.1°, 28.0°, 35.3°, 45.0° and 52.2°, which confirms its crystalline nature. The most intense peak at 22.1° indicates a highly ordered lattice structure. The presence of multiple sharp peaks also suggests high crystallinity and minimal amorphous content. Furthermore, the absence of peak broadening or halo patterns confirms that Bacopasaponin predominantly exists in a pure, crystalline form with little structural disorder. These findings are consistent with the DSC analysis, which also revealed a sharp melting endotherm, providing additional evidence for the crystalline nature of the compound. The crystalline structure of Bacopasaponin c is expected to contribute to its low aqueous solubility and limited bioavailability.

Table 2 Data of XRD pattern of Bacopasaponin C

Sr. No.	2θ (Degree)	Intensity (a.u.)	Relative Intensity (%)	d-spacing (Å)	Remark
1	15.2	180	72.0	5.82	Characteristic peak
2	22.1	250	100.0	4.02	Highest intensity peak
3	28.0	140	56.0	3.18	Crystalline peak
4	35.3	130	52.0	2.54	Moderate peak
5	45.0	100	40.0	2.01	Minor peak
6	52.2	90	36.0	1.75	Minor peak

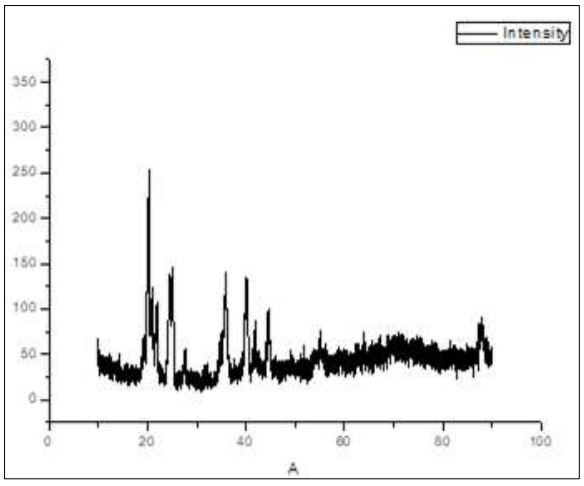


Fig. 9. XRD pattern of Bacopasaponin C

3.21.2. XRD of Asiatic acid

The X-ray diffraction pattern of (Table 3, Fig. 10) Asiatic acid showed clear, sharp peaks at particular 2θ values, which confirms its crystalline nature. The presence of intense peaks at 14.8°, 18.5°, 21.9° and 26.4°, 31.2°, 34.8° suggests an ordered lattice structure. The most prominent peak at 21.9° suggests that this crystallographic plane dominates the diffraction pattern. The sharpness and high intensity of the peaks suggest a large crystallite size and minimal amorphous content, which confirms the purity of the compound. The absence of peak broadening further supports the well-defined crystalline structure of asiatic acid.

Table 3 Data of XRD pattern of Asiatic acid

Sr. No.	2θ (Degree)	Intensity (a.u.)	Relative Intensity (%)	d-spacing (Å)	Remark
1	14.8	160	64.0	5.97	Characteristic peak
2	18.5	210	84.0	4.79	Sharp peak
3	21.9	250	100.0	4.05	Highest intensity peak
4	26.4	180	72.0	3.37	Crystalline peak
5	31.2	140	56.0	2.86	Moderate peak
6	34.8	120	48.0	2.57	Minor peak

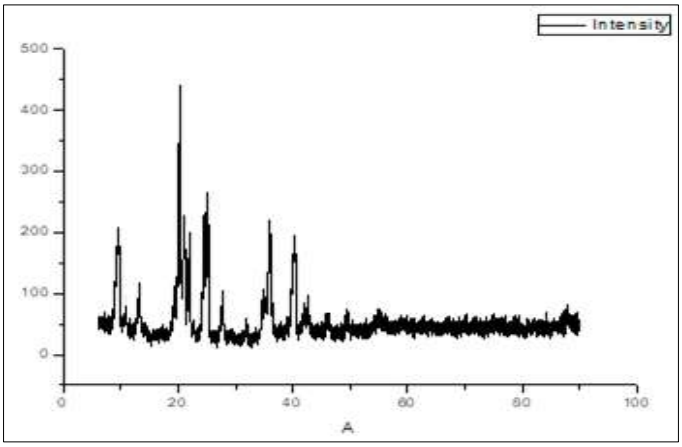


Fig. 10. XRD pattern of Asiatic acid

3.21.3. XRD analysis of Optimized Phytosomal Formulation

The X-ray diffraction pattern of the optimised phytosomal formulation (Table 4, Fig. 11) showed a marked decrease in the intensity and sharpness of the characteristic peaks compared with the pure phytoconstituents (Asiatic acid and Bacopasaponin c). The distinct crystalline peaks observed in the pure drugs were found to be broadened, shifted or completely absent in the formulation, indicating a transformation in the solid-state properties. The appearance of a broad halo pattern in the 15°-30° (2θ) region suggests that the crystalline drugs have converted into an amorphous or molecularly dispersed form within the phospholipid matrix. This change is attributed to strong interactions between the drug and phospholipids, leading to the formation of a stable phytosomal complex. The reduction in peak intensity and the absence of sharp diffraction peaks confirm a loss of long-range order and decreased crystallinity, which are key indicators of successful phytosome formation. Additionally, the absence of new peaks indicates that no chemical incompatibility or degradation occurred during formulation. XRD analysis confirms that the optimised phytosomal formulation exists in a partially or completely amorphous state, which is expected to enhance the solubility, dissolution rate and bioavailability of the phytoconstituents.

Table 4 Data of XRD pattern of Phytosomal Formulation

Sr. No.	2θ (Degree)	Intensity (a.u.)	Relative Intensity (%)	d-spacing (Å)	Remark
1	16.2	80	65.0	5.47	Broad peak
2	21.5	95	100.0	4.13	Diffused peak

Sr. No.	2θ (Degree)	Intensity (a.u.)	Relative Intensity (%)	d-spacing (Å)	Remark
3	26.8	70	73.6	3.32	Reduced intensity
4	31.4	45	47.3	2.84	Minor peak
5	35.6	35	36.8	2.52	Weak peak

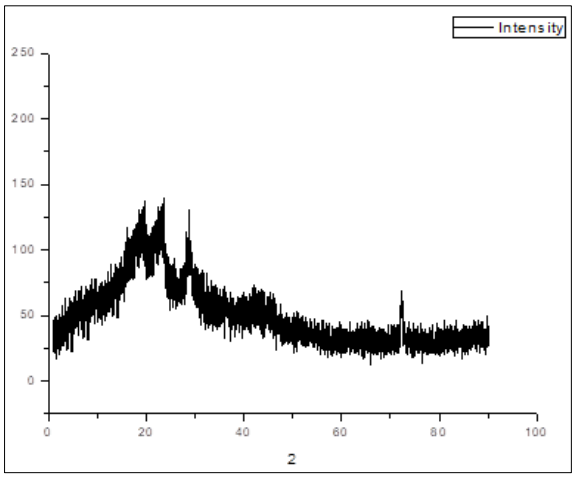


Fig. 11. XRD pattern of Optimized Phytosomal Formulation

4. CONCLUSION

Using a phospholipid-based nano-delivery technology, the current study efficiently developed and defined dual-component herbal phytosomes containing Bacopasaponin C and Asiatic acid. Favorable physicochemical characteristics, such as ideal particle size, increased entrapment efficiency, and better stability profiles, were displayed by the prepared phytosomes. The formulation's appropriateness for extended therapeutic action was confirmed by *in vitro* release tests, which showed a sustained and regulated release pattern. When compared to traditional formulations, the solubility and dispersion properties of both phytoconstituents were greatly improved by their integration into the phytosomal system. Additionally, the problems related to low bioavailability and quick degradation of herbal bioactives may be addressed by the nano-phytosomal method. The developed dual-herbal phytosomal delivery system represents a promising strategy for improving the therapeutic efficacy and pharmacokinetic performance of plant-derived compounds.

Acknowledgements

We are thankful to the management and principal Y.B. Chavan College of Pharmacy, Aurangabad (M.S.), India, for providing the facilities and infrastructure for carrying out the research work.

Funding

No funds, grants, or other support was received.

Authorship contribution statement

Momin Subura Mohd Riyaz: Conceptualization, Investigation, Writing-original draft, Data curation; Subur W Khan: Writing-review and editing, Data Curation, Visualization, Validation, Analysis and Data Curation.

Data availability

All data generated or analyzed during this study are included in this article.

Ethics declarations

Ethics approval and consent to participate

Not applicable.

Consent for publication

Not applicable.

Competing interests

The authors have no relevant financial or non-financial interests to disclose.

REFERENCES

[1] Jaiswal P, et al. Development of self-microemulsifying drug delivery system and solid-self-microemulsifying drug delivery system of telmisartan. Int J Pharm Investig. 2014;4(4):195-206.

[2] Semalty A, et al. Supramolecular phospholipids-polyphenolics interactions: the PHYTOSOME® strategy to improve the bioavailability of phytochemicals. Fitoterapia. 2010;81(5):306-314.

[3] Kidd PM. Bioavailability and activity of phytosome complexes from botanical polyphenols: the silymarin, curcumin, green tea, and grape seed extracts. Altern Med Rev. 2009;14(3):226-246.

[4] Gray NE, et al. Centella asiatica: phytochemistry and mechanisms of neuroprotection and cognitive enhancement. Phytochem Rev. 2018;17(1):161-194.

[5] Aguiar S, Borowski T. Neuropharmacological review of the nootropic herb Bacopa monnieri. Rejuvenation Res. 2013;16(4):313-326.

[6] Russo A, Borrelli F. Bacopa monniera, a reputed nootropic plant: an overview. Phytomedicine. 2005;12(4):305-317.

[7] Kongkeaw C, et al. Meta-analysis of randomized controlled trials on cognitive effects of Bacopa monnieri extract. J Ethnopharmacol. 2014;151(1):528-535.

[8] Nagoor Meeran MF, et al. Pharmacological properties, molecular mechanisms, and pharmaceutical development of Asiatic acid: a pentacyclic triterpenoid of therapeutic promise. Front Pharmacol. 2018;9:892.

[9] Lu M, et al. Phyto-phospholipid complexes (phytosomes): a novel strategy to improve the bioavailability of active constituents. Asian J Pharm Sci. 2019;14(3):265-274.

[10] KS S, Aditi K. Phytosome as a novel drug delivery system for bioavailability enhancement of phytoconstituents and its applications: a review. J Drug Delivery Ther. 2021;11(3):1-10.

[11] Srivastava N, et al. Development and validation of UV spectrophotometric method for the quantitative estimation of quercetin in bulk followed by its solubility studies. J Appl Spectrosc. 2024;91:700-708.

[12] Dowell A, Davidson G, Ghosh D. Validation of quantitative HPLC method for bacosides in keenmind. Evid Based Complement Altern Med. 2015;2015:696172.

[13] Arthy JV, et al. Analytical method development of bioactive compounds in Bacopa monnieri leaf extract by RP-HPLC. Int J Multidiscip Res. 2025;7(2):1-7.

[14] Varsha M, Devika R. Formulation and evaluation of phytosome, a novel biomedicine. Int J Pharm Sci Rev Res. 2023;79(1):06.

[15] Khan FN, Khan S. QbD-engineered development and in vivo evaluation of an Articaine-loaded nanostructured lipid carrier in situ gel: a painless drug delivery platform for sustained periodontal anesthesia. Next Nanotechnol. 2026;9:100426.

[16] Chate MD, et al. Design and validation of a stability-indicating RP-HPLC technique for quantifying ivacaftor in bulk and commercial formulations. Curr Pharm Anal. 2025;21(4):216-224.

[17] Hebbar S, et al. RP-HPLC method development and validation of Asiatic acid isolated from the plant Centella asiatica. Int J Appl Pharm. 2019;11:72-78.

[18] Chysirichote T, Wattanasiriwit W, Uraipong C. Optimization of ethanolic extraction of asiaticoside and asiatic acid: a stability study and correlation of dielectric constant. Appl Food Res. 2025;5(1):100899.

[19] Handayani DP, et al. Extraction of Centella asiatica herb using microwave-assisted solvent extraction: optimization of crude extract using Box-Behnken design. Green Anal Chem. 2024;11:100146.

Supplementary Tables and Figures

Table S1 Designed batches of Phytosomes

Ingredients	B1	B2	B3	B4	B5	B6	B7	B8
Centellaasiatica(mg)	50	50	50	50	50	50	50	50
Bacopamonieri(mg)	50	50	50	50	50	50	50	50
Conc. of Soya lecithin (mg)	200	100	200	100	100	200	100	200
Temperature (℃)	70	50	50	70	50	70	70	50
Time (Min)	150	150	150	90	90	90	150	90
Dichloromethane (ml)	40	40	40	40	40	40	40	40
N-Hexane (ml)	10	10	10	10	10	10	10	10

Table S2 Factorial design for Phytosomal formulation

		Factor 1	Factor 2	Factor 3	Response 1	Response 2
Std	Run	A:Concentration of Soya Lecithin	B:Temperature	C:Time	Particle Size	Percent Drug Release
		mg	Degree	Min	nm	%
8	1	200	70	150	352.13	82.23
5	2	100	50	150	337.02	90.22
6	3	200	50	150	429.21	76.31
3	4	100	70	90	352.16	88.46
1	5	100	50	90	421.11	82.14
4	6	200	70	90	452.32	74.10
7	7	100	70	150	246.14	95.85
2	8	200	50	90	498.06	68.21

Table S3 Standard concentration for Asiatic acid calibration curve

Concentrations (µg/ml)	Absorbance
2	0.243
4	0.456
6	0.634
8	0.845
10	1.014
12	1.236

Table S4 Standard concentration for Bacopasaponin C calibration curve

Concentrations (µg/ml)	Absorbance
5	0.068
10	0.254
15	0.463
20	0.638
25	0.872
30	1.056

Table S5 Drug content analysis

Batch	Drug Content (%)
B1	88.42
B2	91.36
B3	85.27
B4	89.75
B5	86.94
B6	84.63
B7	93.12
B8	82.48

Natural Resources for Human Health
eISSN: 2583-1194

Table S6 Entrapment efficiency of Phytosomes

Batch	Entrapment Efficiency (%)
B1	78.45
B2	84.12
B3	74.36
B4	81.28
B5	79.63
B6	73.54
B7	88.96
B8	71.22

Table S7 Particle size of Designed Batches

Batch	Particle Size (nm)	PDI
B1	352.13	0.274
B2	337.02	0.262
B3	429.21	0.238
B4	352.16	0.273
B5	421.11	0.270
B6	452.32	0.295
B7	246.14	0.270
B8	498.06	0.278

Table S8 Zeta Potential of Designed Batches

Batch	Zeta Potential (mV)
B1	-28.45
B2	-32.16
B3	-25.36
B4	-30.22
B5	-27.84

Batch	Zeta Potential (mV)
B6	-24.91
B7	-34.69
B8	-22.73

Table S9 *In vitro* release study of Phytosomal Formulation

Time (Hrs)	B1	B2	B3	B4	B5	B6	B7	B8
0	0	0	0	0	0	0	0	0
1	18.25 ± 2.1	22.14 ± 2.0	15.22 ± 2.3	20.45 ± 2.2	17.86 ± 2.1	14.32 ± 2.4	25.36 ± 1.9	12.14 ± 2.5
2	28.46 ± 1.9	35.62 ± 1.8	25.44 ± 2.1	33.28 ± 1.9	27.54 ± 2.0	23.76 ± 2.2	40.12 ± 1.7	20.36 ± 2.3
4	45.12 ± 2.3	52.33 ± 2.2	40.11 ± 2.5	50.16 ± 2.1	43.32 ± 2.3	38.45 ± 2.5	58.44 ± 2.0	34.18 ± 2.6
6	58.34 ± 1.8	66.45 ± 1.9	52.67 ± 2.0	63.72 ± 1.8	55.18 ± 1.9	49.87 ± 2.1	72.68 ± 1.8	45.27 ± 2.2
8	66.75 ± 2.0	75.86 ± 1.7	60.32 ± 1.9	72.14 ± 1.7	63.45 ± 1.8	57.23 ± 1.9	82.35 ± 1.6	52.41 ± 2.0
12	74.21 ± 1.7	83.21 ± 1.6	68.45 ± 1.8	80.36 ± 1.6	71.28 ± 1.7	65.18 ± 1.8	90.14 ± 1.5	60.35 ± 1.9
24	82.23 ± 1.5	90.22 ± 1.4	76.31 ± 1.6	88.46 ± 1.5	82.14 ± 1.6	74.10 ± 1.7	95.85 ± 1.3	68.21 ± 1.8

Table S10 Information of Factorial design

File Version	13.0.5.0		
Study Type	Factorial	**Subtype**	Randomized
Design Type	2 Level Factorial	**Runs**	8.00
Design Model	3FI	**Blocks**	No Blocks
Center Points	0.0000	**Build Time (ms)**	13.00

Natural Resources for Human Health
eISSN: 2583-1194

Table S11 Factors for the factorial design

Factor	Name	Units	Type	SubType	Minimum	Maximum	Coded Low	Coded High	Mean	Std. Dev.
A	Concentration of Soya Lecithin	mg	Numeric	Continuous	100.00	200.00	-1 ↔ 100.00	+1 ↔ 200.00	150.00	53.45
B	Temperature	Degree	Numeric	Continuous	50.00	70.00	-1 ↔ 50.00	+1 ↔ 70.00	60.00	10.69
C	Time	Min	Numeric	Continuous	90.00	150.00	-1 ↔ 90.00	+1 ↔ 150.00	120.00	32.07

Table S12 ANOVA data for response Particle size

Source	Sum of Squares	df	Mean Square	F-value	p-value	
Model	44296.71	6	7382.79	667.01	0.0296	significant
A-Concentration of Soya Lecithin	17605.32	1	17605.32	1590.58	0.0160	
B-Temperature	9986.38	1	9986.38	902.23	0.0212	
C-Time	16123.59	1	16123.59	1456.71	0.0167	
AB	171.22	1	171.22	15.47	0.1585	
AC	55.49	1	55.49	5.01	0.2674	
BC	354.71	1	354.71	32.05	0.1113	
Residual	11.07	1	11.07			
Cor Total	44307.78	7				

Table S13 Fit Statistic data for response Particle size

Std. Dev.	3.33	**R^2**	0.9998
Mean	386.02	**Adjusted R^2**	0.9983
C.V. %	0.8619	**Predicted R^2**	0.9840
		Adeq Precision	81.7054

Natural Resources for Human Health
eISSN: 2583-1194

Table S14 Data for Coefficients in Terms of Coded Factors for response Particle size

Factor	Coefficient Estimate	df	Standard Error	95% CI Low	95% CI High	VIF
Intercept	386.02	1	1.18	371.07	400.96	
A-Concentration of Soya Lecithin	46.91	1	1.18	31.97	61.86	1.0000
B-Temperature	-35.33	1	1.18	-50.28	-20.39	1.0000
C-Time	-44.89	1	1.18	-59.84	-29.95	1.0000
AB	4.63	1	1.18	-10.32	19.57	1.0000
AC	2.63	1	1.18	-12.31	17.58	1.0000
BC	-6.66	1	1.18	-21.60	8.29	1.0000

Table S15 Data of Analysis of variance for the response percentage of drug release

Source	Sum of Squares	df	Mean Square	F-value	p-value	
Model	585.79	6	97.63	1506.67	0.0197	significant
A-Concentration of Soya Lecithin	389.48	1	389.48	6010.56	0.0082	
B-Temperature	70.57	1	70.57	1089.00	0.0193	
C-Time	125.61	1	125.61	1938.45	0.0145	
AB	0.0024	1	0.0024	0.0378	0.8777	
AC	0.0722	1	0.0722	1.11	0.4828	
BC	0.0544	1	0.0544	0.8403	0.5277	
Residual	0.0648	1	0.0648			
Cor Total	585.86	7				

Table S16 Fit Statistic Data for response percent drug release

Std. Dev.	0.2546	**R^2**	0.9999
Mean	82.19	**Adjusted R^2**	0.9992
C.V. %	0.3097	**Predicted R^2**	0.9929
		Adeq Precision	116.8330

Table S17 Coefficients in Terms of Coded Factors for response percent drug release

Factor	Coefficient Estimate	df	Standard Error	95% CI Low	95% CI High	VIF
Intercept	82.19	1	0.0900	81.05	83.33	
A-Concentration of Soya Lecithin	-6.98	1	0.0900	-8.12	-5.83	1.0000
B-Temperature	2.97	1	0.0900	1.83	4.11	1.0000
C-Time	3.96	1	0.0900	2.82	5.11	1.0000
AB	-0.0175	1	0.0900	-1.16	1.13	1.0000
AC	0.0950	1	0.0900	-1.05	1.24	1.0000
BC	-0.0825	1	0.0900	-1.23	1.06	1.0000

Table S18 Preferable solutions of optimizations

Number	Concentration of Soya Lecithin	Temperature	Time	Particle Size	Percent Drug Release	Desirability	
1	**100.614**	**69.991**	**149.999**	**245.671**	**95.853**	**1.000**	**Selected**
2	100.137	69.971	149.862	245.497	95.895	1.000	
3	100.104	69.952	149.579	246.060	95.859	1.000	
4	100.003	69.790	149.979	245.982	95.876	1.000	
5	100.298	69.838	149.991	246.055	95.851	1.000	
6	101.102	69.999	150.000	246.163	95.788	0.999	
7	100.005	69.640	150.000	246.646	95.835	0.999	
8	101.176	70.000	150.000	246.239	95.778	0.998	
9	100.000	70.000	148.989	246.790	95.812	0.998	
10	101.798	70.000	150.000	246.912	95.692	0.996	
11	100.000	69.988	148.427	247.861	95.738	0.995	
12	100.000	70.000	148.067	248.455	95.696	0.993	
13	100.000	70.000	147.799	248.939	95.662	0.991	
14	103.027	70.000	150.000	248.244	95.522	0.990	
15	100.000	70.000	147.510	249.462	95.626	0.989	
16	100.000	68.938	149.999	249.918	95.631	0.989	

17	100.000	69.969	147.216	250.132	95.580	0.987	
18	100.000	70.000	146.977	250.424	95.559	0.986	
19	100.000	68.653	150.000	251.244	95.549	0.984	
20	104.118	69.946	150.000	249.677	95.356	0.984	
21	100.000	68.513	150.000	251.897	95.508	0.982	
22	104.721	70.000	150.000	250.079	95.288	0.982	
23	100.002	70.000	146.212	251.808	95.462	0.982	
24	102.977	70.000	148.350	251.161	95.321	0.980	
25	100.000	70.000	145.670	252.784	95.394	0.979	
26	105.664	70.000	149.999	251.102	95.158	0.978	
27	100.000	68.092	150.000	253.858	95.386	0.976	
28	100.000	67.865	150.000	254.915	95.320	0.973	
29	106.854	70.000	150.000	252.391	94.994	0.972	
30	107.377	70.000	149.999	252.958	94.922	0.970	
31	107.753	70.000	150.000	253.365	94.870	0.968	
32	100.000	69.830	143.631	257.235	95.087	0.964	
33	100.000	70.000	142.648	258.242	95.012	0.961	
34	100.000	66.987	150.000	259.010	95.065	0.960	
35	110.636	70.000	150.000	256.487	94.472	0.955	
36	100.001	70.000	141.353	260.583	94.849	0.953	
37	100.000	66.003	150.000	263.598	94.779	0.946	
38	100.000	70.000	139.954	263.110	94.672	0.945	
39	100.000	70.000	139.330	264.236	94.594	0.941	
40	113.705	70.000	150.000	259.813	94.049	0.940	
41	100.000	65.098	149.999	267.818	94.516	0.933	
42	100.000	69.999	137.143	268.191	94.318	0.928	
43	116.296	70.000	150.000	262.620	93.691	0.928	
44	118.042	70.000	150.000	264.511	93.450	0.920	

45	100.000	70.000	135.397	271.341	94.098	0.918	
46	100.248	70.000	129.524	282.208	93.322	0.882	
47	100.000	61.577	150.000	284.231	93.493	0.881	
48	100.000	60.919	149.998	287.302	93.302	0.871	
49	130.440	70.000	150.000	277.944	91.739	0.862	
50	100.000	59.918	150.000	291.963	93.011	0.857	
51	100.001	70.000	120.527	298.199	92.221	0.830	
52	100.000	57.520	149.382	304.087	92.234	0.818	
53	100.000	54.081	150.000	319.174	91.315	0.770	
54	100.000	52.968	150.000	324.363	90.992	0.754	
55	156.156	70.000	150.000	305.805	88.190	0.743	
56	100.000	50.222	150.000	337.161	90.195	0.713	
57	102.453	50.001	150.000	340.394	89.794	0.699	

Table S19 Optimized batch

Concentration of Soya Lecithin (mg)	Temperature (℃)	Time (Min)	Particle Size (nm)	Percent Cumulative Drug Release (%)
100.614	69.991	149.999	245.671	95.853

Table S20 Optimized Batch Final formula

Ingredients	Quantity
Centellaasiatica(mg)	50
Bacopamonieri(mg)	50
Conc. of Soya lecithin (mg)	100.614
Temperature (℃)	69.991
Time (Min)	150.999
Dichloromethane (ml)	40
N-Hexane (ml)	10

Natural Resources for Human Health
eISSN: 2583-1194

Table S21 Evaluation of Optimized Batch

Drug content (%)	Entrapment efficiency (%)	Particle size (nm)	Zeta potential	In-vitro release (%)
94.86	90.64	236.75	-35.23	99.17

Supplementary Figures

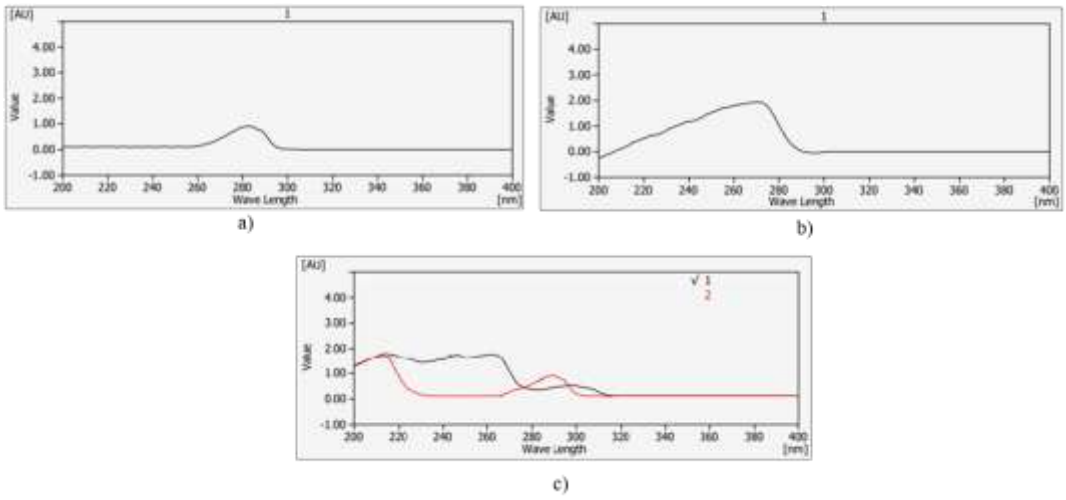


Fig. S1. a) Wavelength maxima of Asiatic acid; b) Wavelength maxima of Bacopasaponin C; c) Isobestic point determination of Asiatic acid and Bacopasaponin C

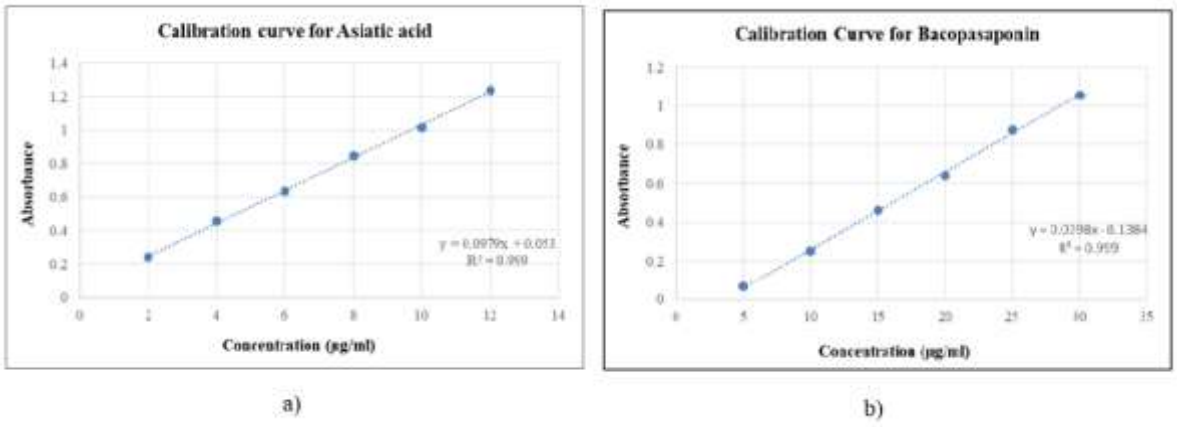
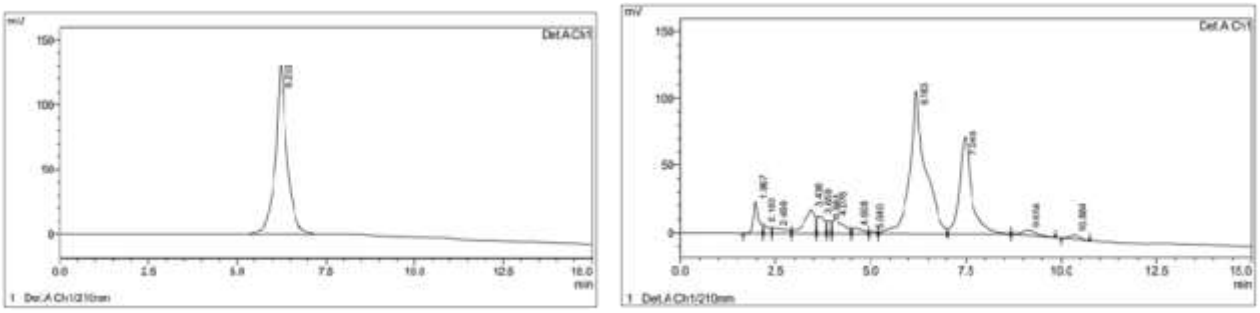


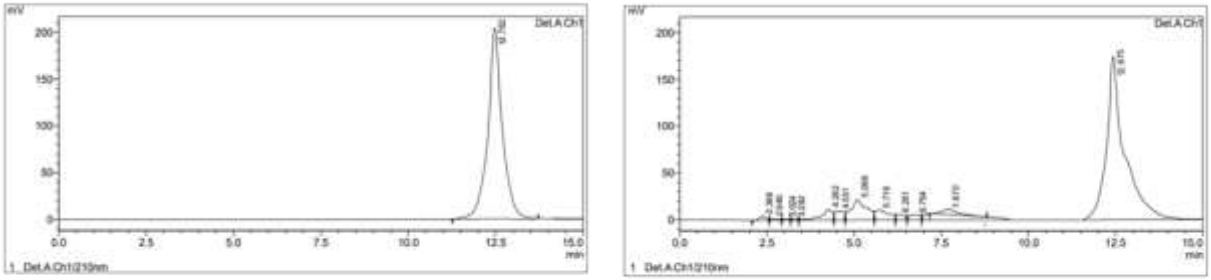
Fig. S2. a) Calibration curve for Asiatic acid; b) Calibration curve for Bacopasaponin

Natural Resources for Human Health
eISSN: 2583-1194



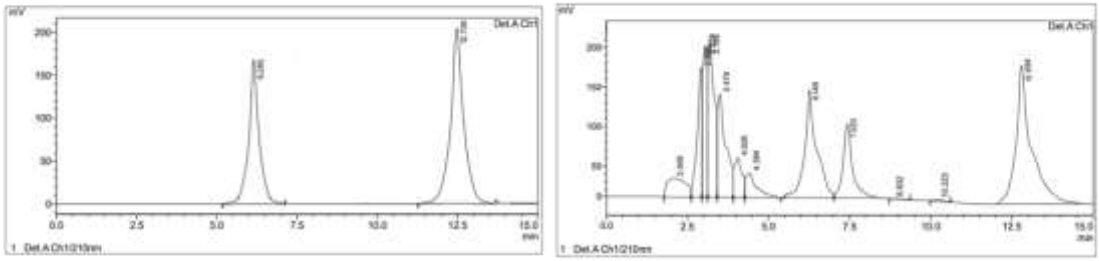
a) b)

Fig. S3. a) Standard Chromatogram of Asiatic acid; b) Chromatogram of Asiatic acid in extract (Sample)



a) b)

Fig. S4. a) Standard Chromatogram of Bacopasaponin; b) Chromatogram of Bacopasaponinin c (Sample)



a) b)

Fig. S5. a) Standard Chromatograms of Asiatic acid and Bacopasaponin; b) chromatograms of samples of Asiatic acid and Bacopasaponin by using RP-HPLC

Natural Resources for Human Health
eISSN: 2583-1194

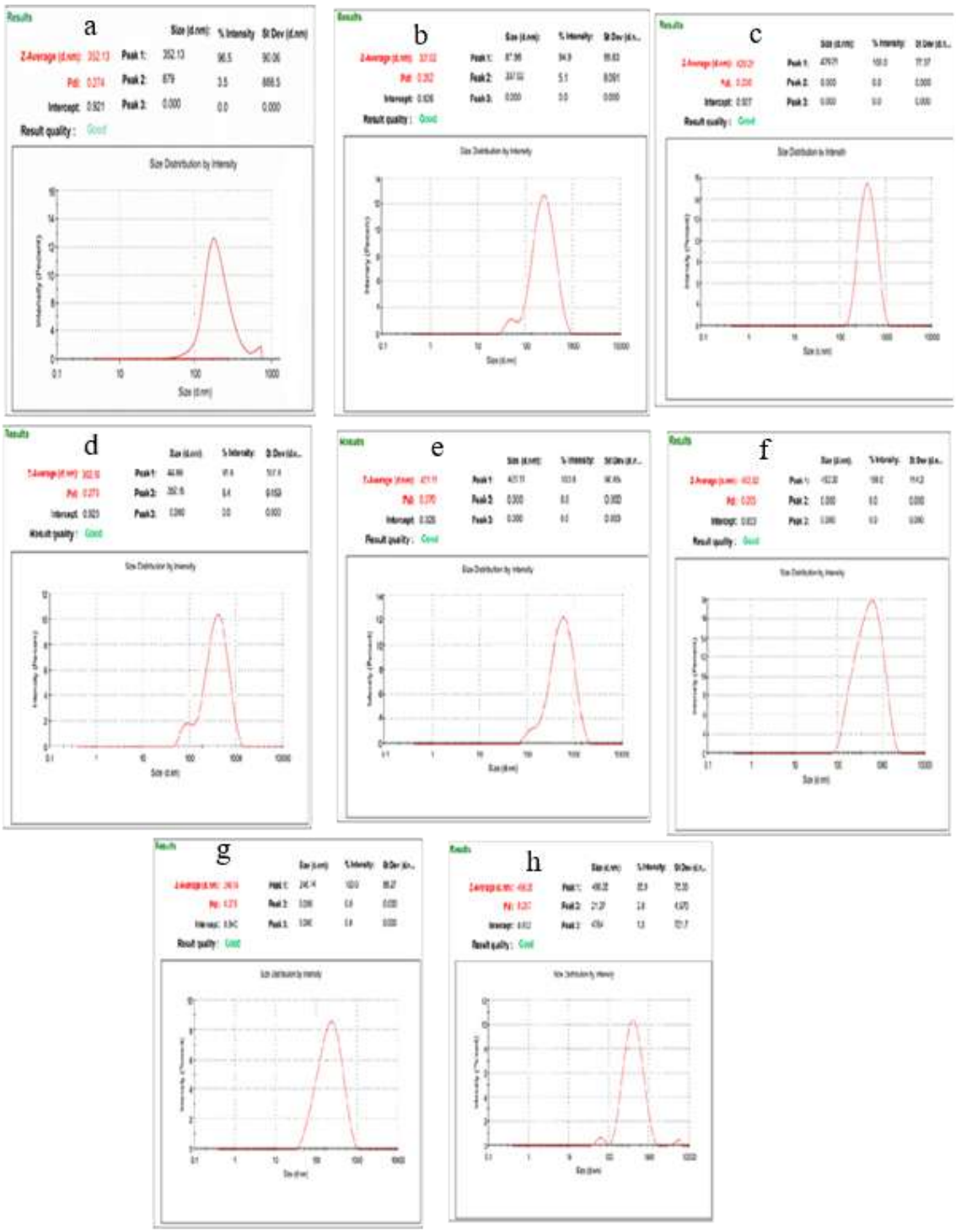


Fig. S6. a) Particle size of Batch B1; b) Particle size of Batch B2; c)Particle size of Batch B3; d) Particle size of Batch B4; e) Particle size of Batch B5; f) Particle size of Batch B6; g) Particle size of Batch B7; h) Particle size of Batch B8

Natural Resources for Human Health
eISSN: 2583-1194

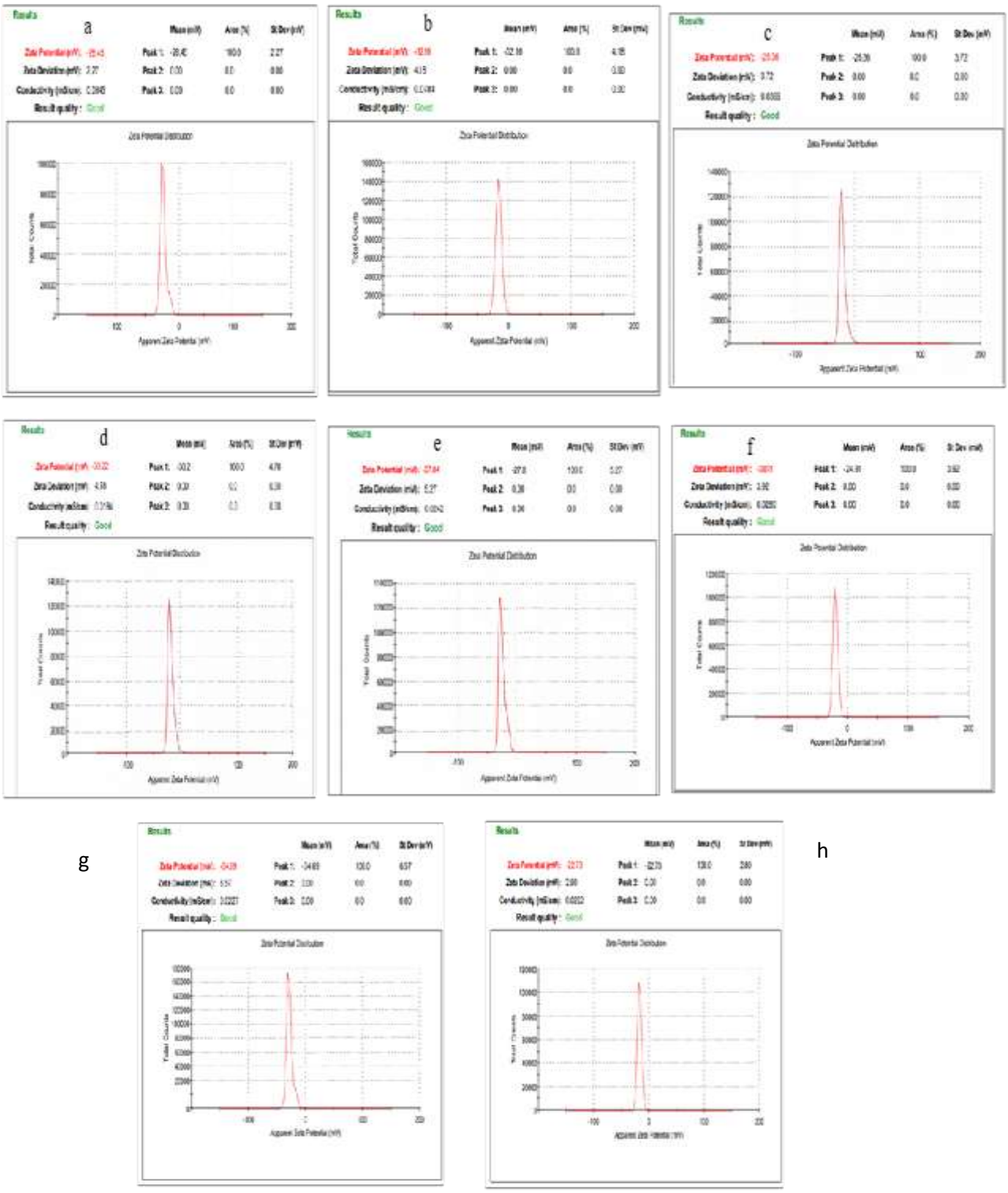


Fig. S7. a) Zeta potential of Batch B1; b) Zeta potential of Batch B2; c) Zeta potential of Batch B3; d) Zeta potential of Batch B4; e) Zeta potential of Batch B5; f) Zeta potential of Batch B6; g) Particle size of Batch B7; h) Particle size of Batch B8

Natural Resources for Human Health
eISSN: 2583-1194

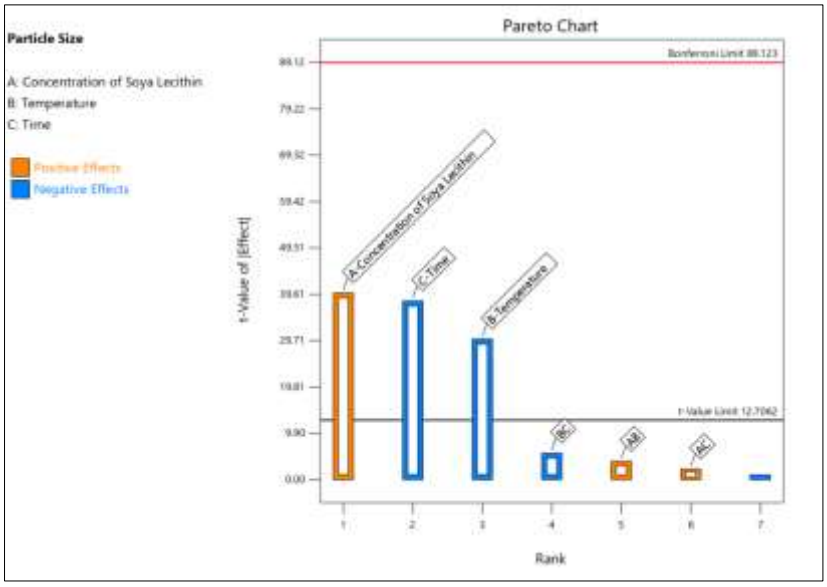


Fig. S8. Pareto chart of Particle size response

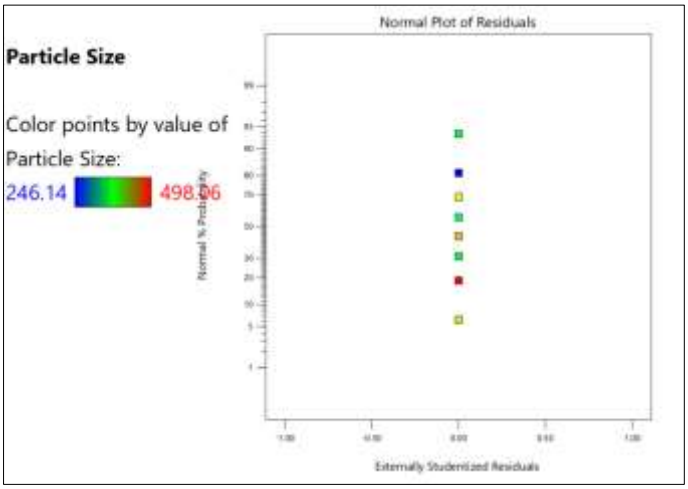


Fig. S9. Normal Plot of Residual for response Particle Size

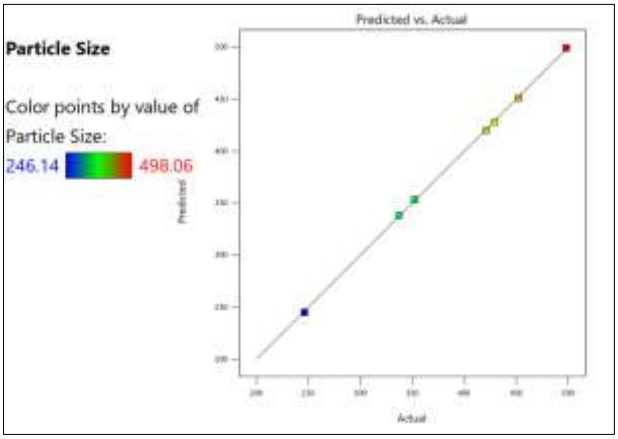


Fig. S10. Predicted vs Actual Data for response Particle Size

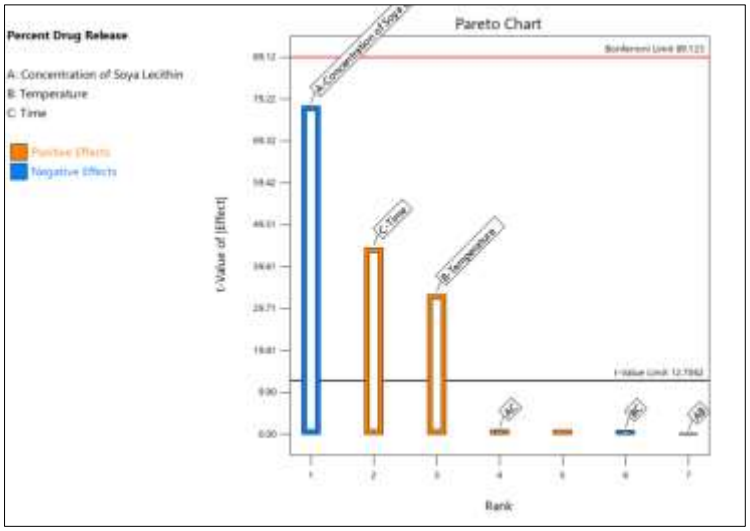


Fig. S11. Pareto graph for response Percent Drug Release

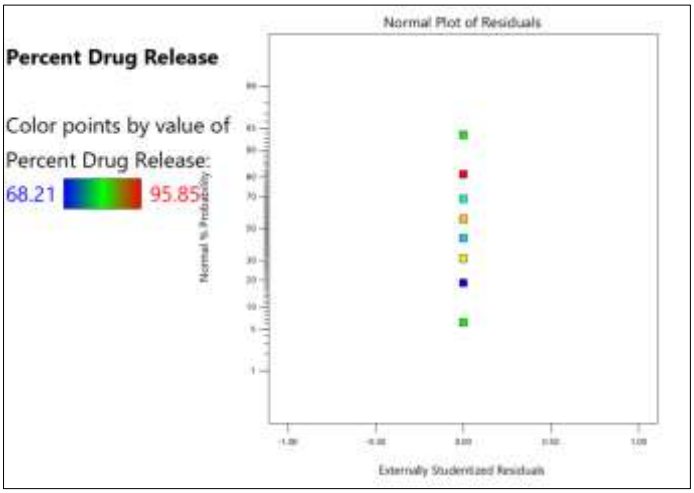


Fig. S12. Normal plot of Residuals for response percent drug release

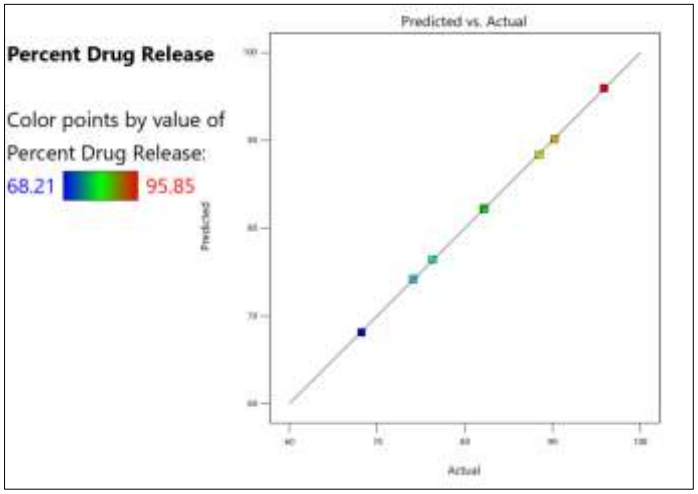


Fig. S13. Predicted vs Actual data for response percent drug release

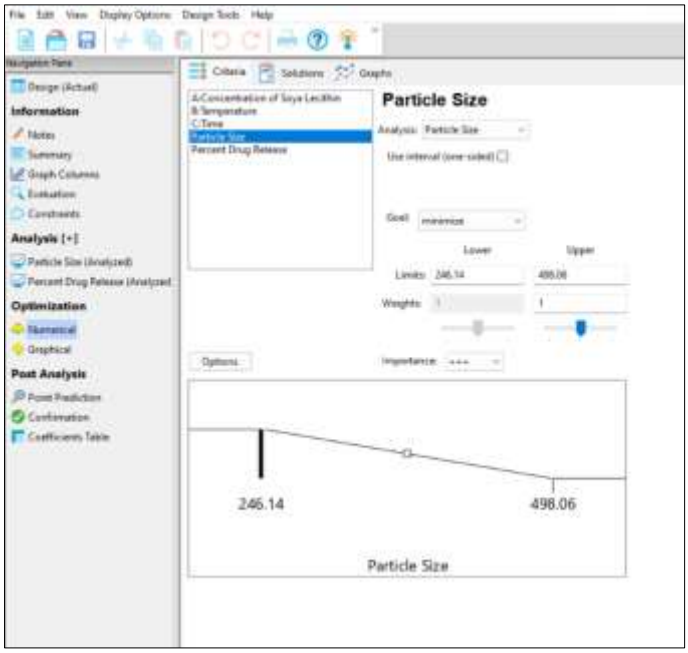


Fig. S14. Optimization criteria for Response Particle size

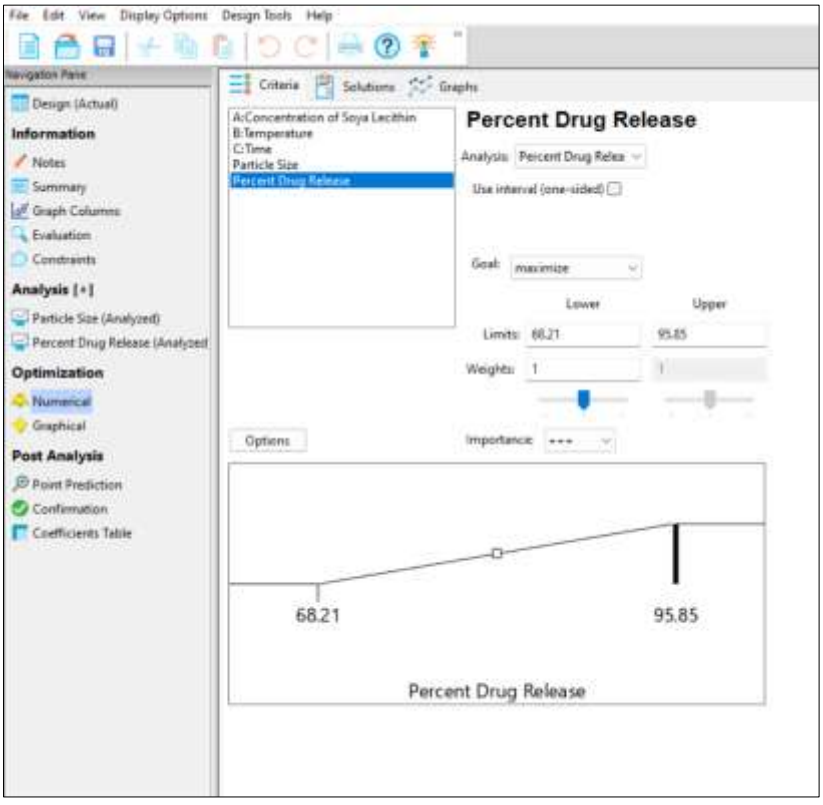


Fig. S15. Optimization criteria for response cumulative percent drug release

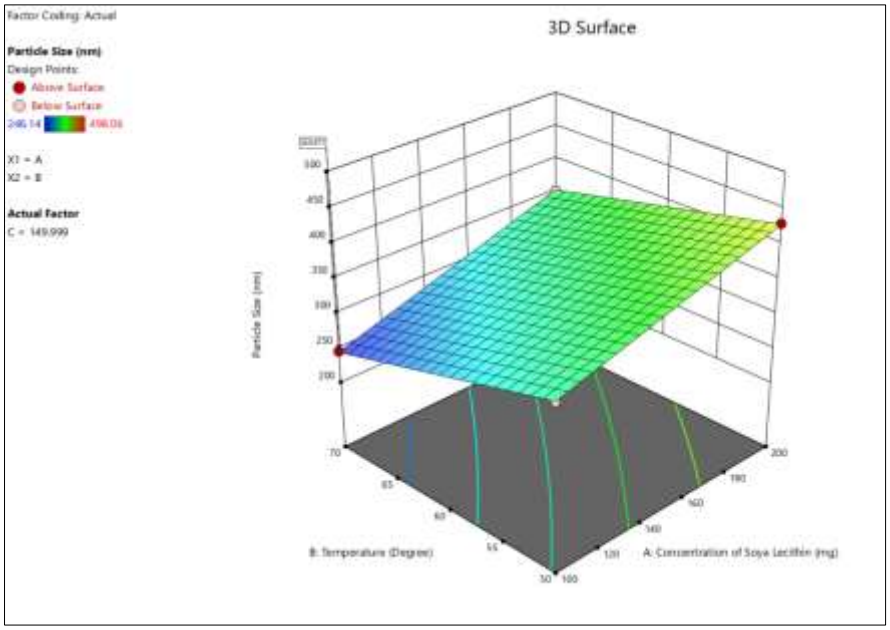


Fig. S16. 3D surface of graph of Concentration of Soya Lecithin and Temperature on Particle Size

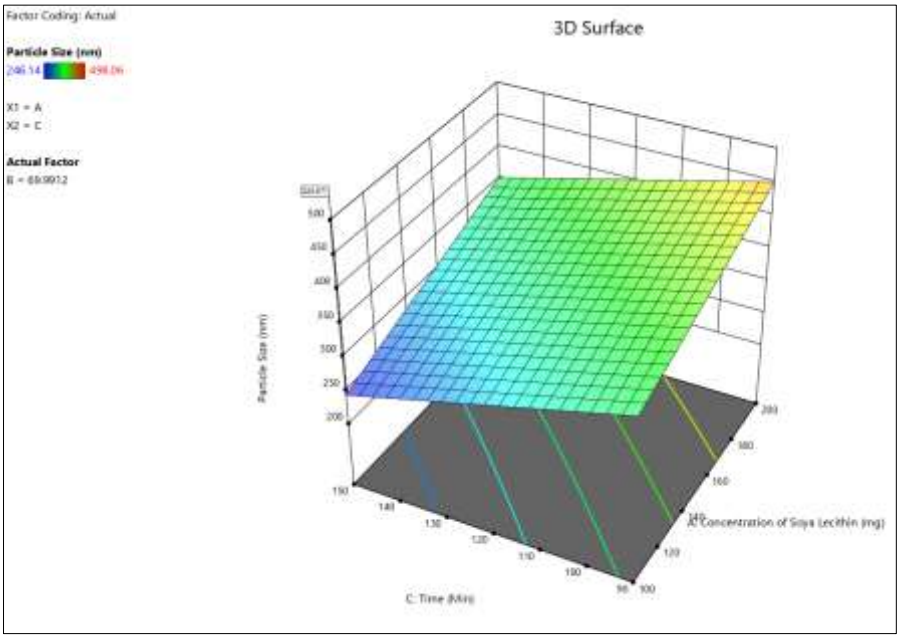


Fig. S17. 3D surface of graph of Effect of Concentration of Soya Lecithin and Time on Particle Size

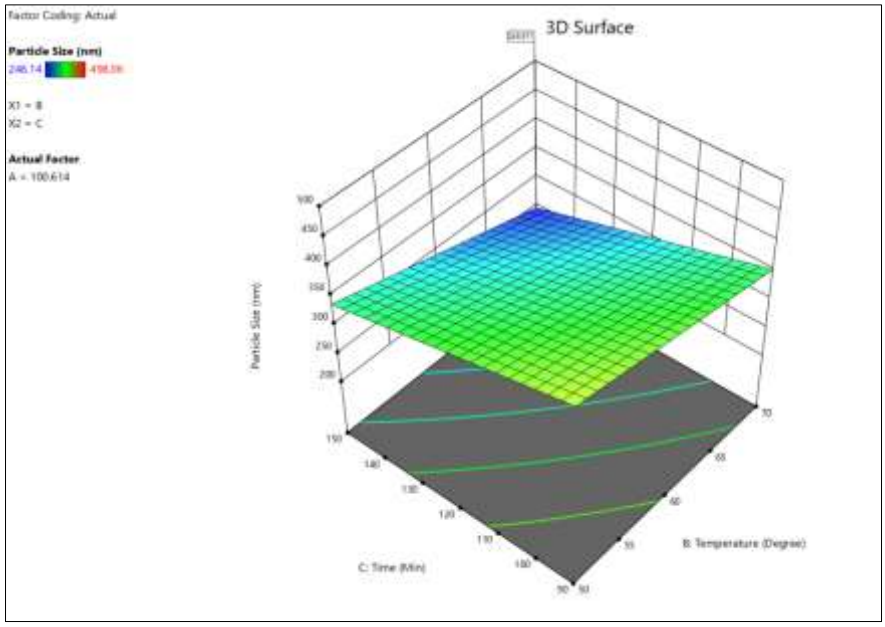


Fig. S18. 3D surface of graph of Effect of Temperature and Time on Particle Size

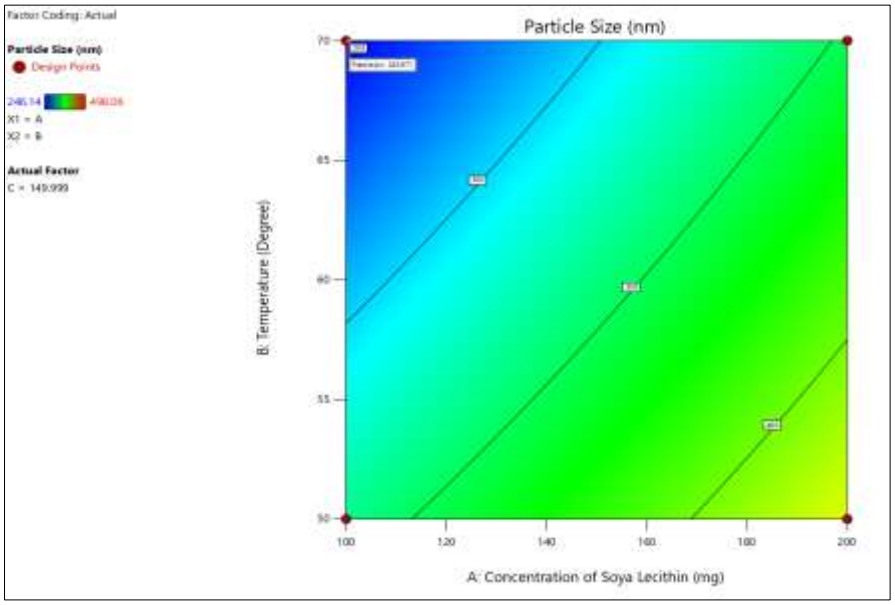


Fig. S19. Counter plot of Concentration of Soya Lecithin and Temperature on Particle Size

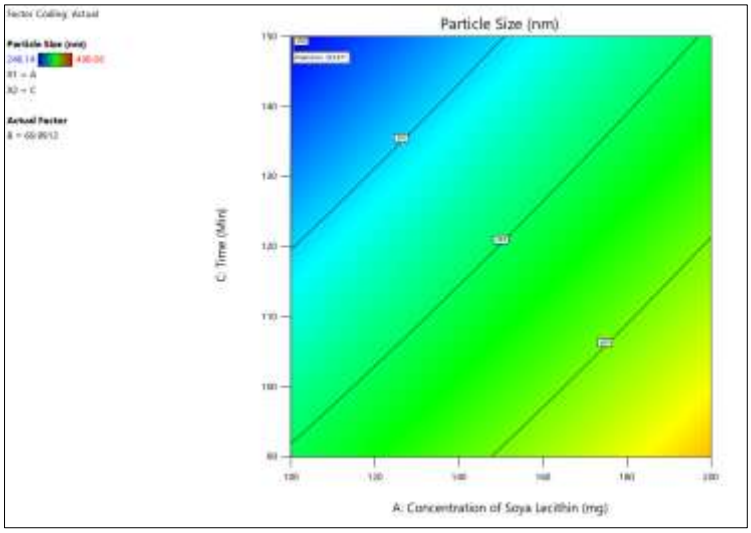


Fig. S20. Counter plot of Concentration of Soya Lecithin and Temperature on Particle Size

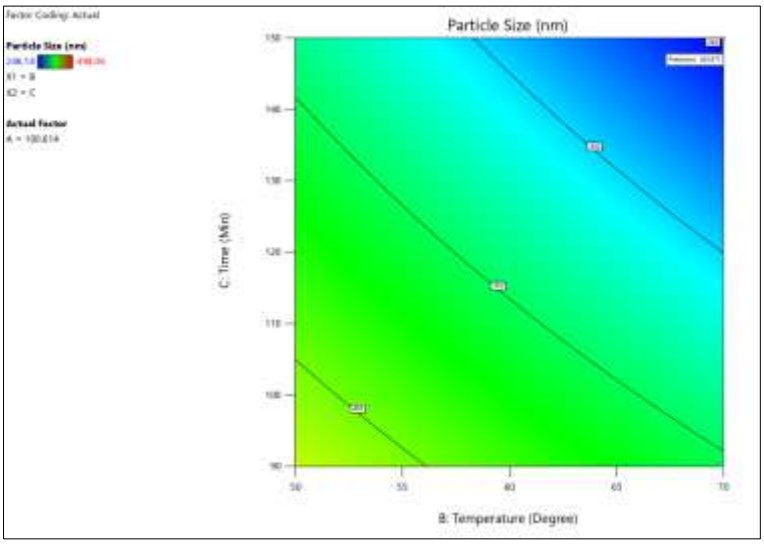


Fig. S21. Counter plot of Temperature and Time on Particle Size

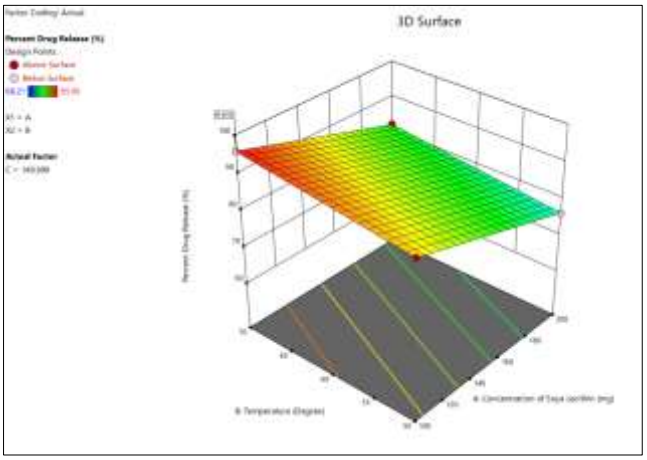


Fig. S22. 3D surface of graph of Effect of Concentration of Soya Lecithin and Temperature on percent drug release

Natural Resources for Human Health
eISSN: 2583-1194

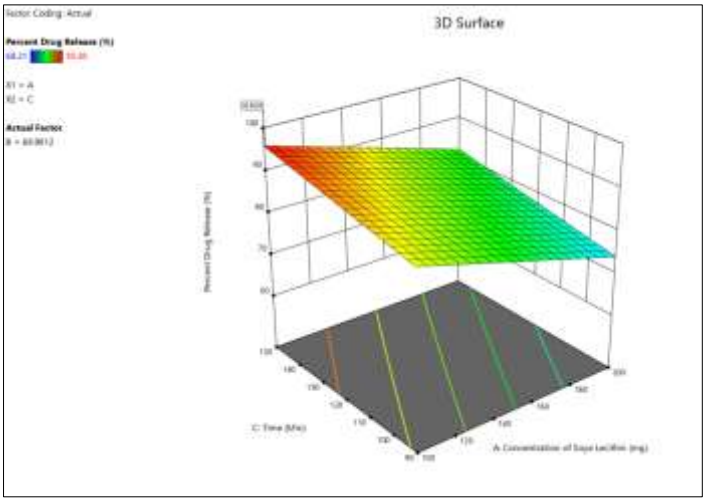


Fig. S23. 3D surface of graph of Effect of Concentration of Soya Lecithin and Time on percent drug release

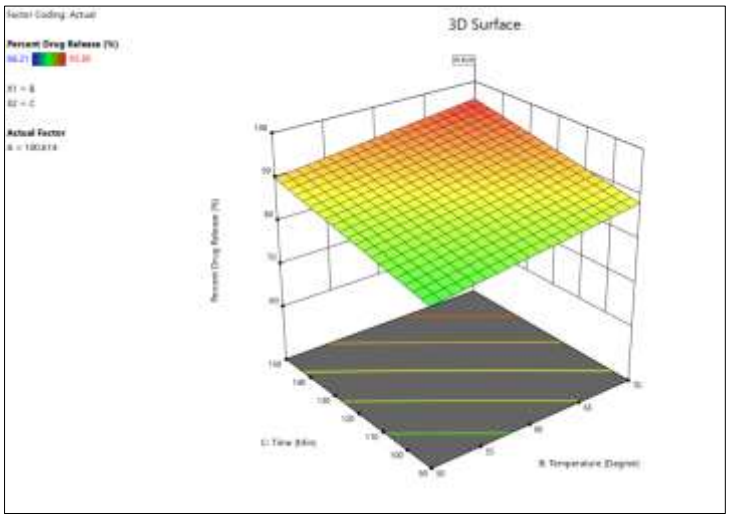


Fig. S24. 3D surface of graph of Effect of Concentration of Temperature and Time on percent drug release

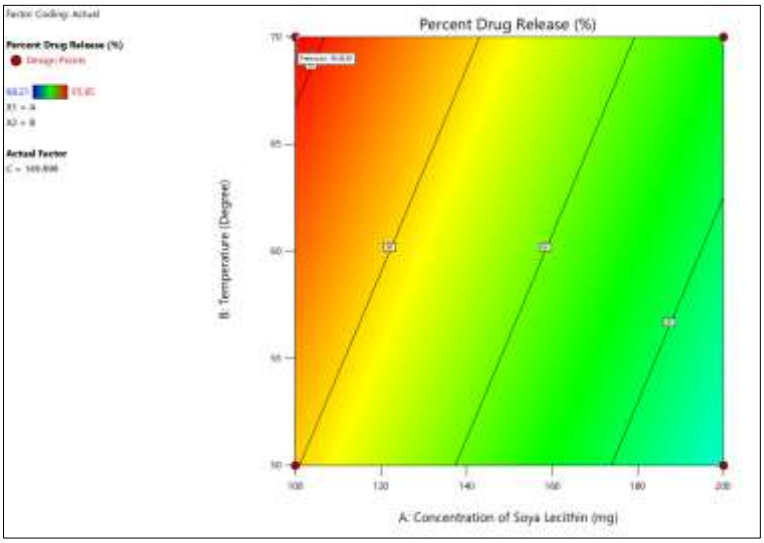


Fig. S25. Counter plot of Concentration of Soya Lecithin and Temperature on Percent Drug Release (%)

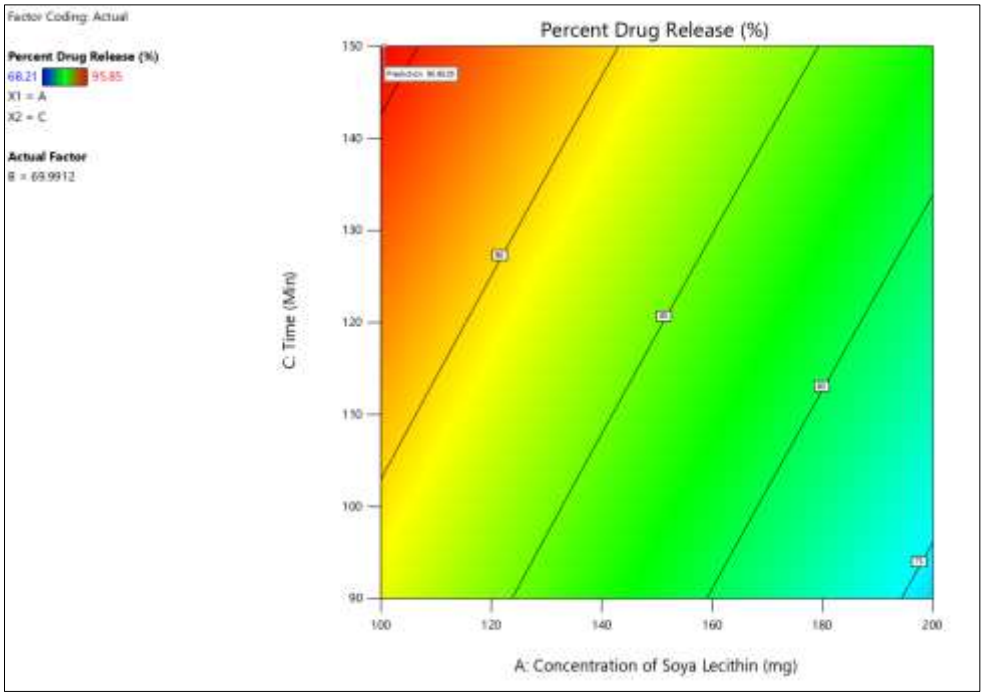


Fig. S26. Counter plot of Concentration of Soya Lecithin and Time on Percent Drug Release (%)

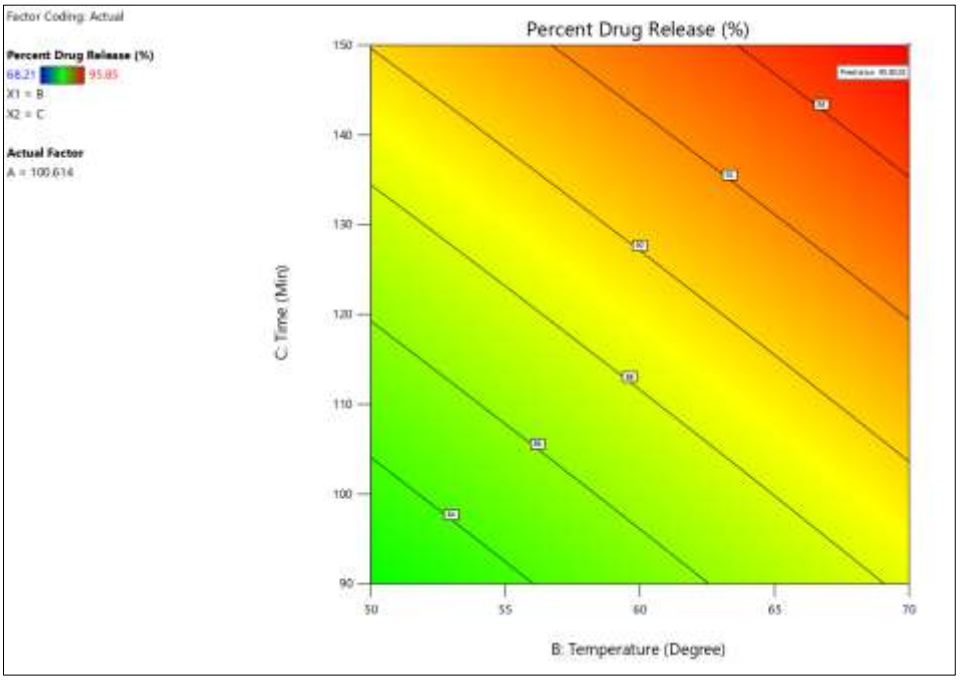


Fig. S27. Counter plot of Temperature and Time on Percent Drug Release (%)